The role of inducible T-cell costimulator in antitumor T cell immunity

Nikoletta Diamantopoulos

Department of Microbiology and Immunology

Faculty of Medicine

Institut de Recherches Cliniques de Montréal (IRCM)

McGill University, Montreal

December 2022

A thesis submitted to McGill University in partial fulfillment of the requirements of the degree of Master of Science (M.Sc.)

Table of Contents

Abstract

Inducible T-cell costimulator (ICOS) is a costimulatory receptor expressed by activated T cells and is essential for T cell activation and function. Its expression has been associated with effective immune checkpoint blockade therapy, and multiple clinical trials targeting ICOS are currently being investigated as a promising cancer immunotherapeutic. However, the role of ICOS in tumor immunity is not fully understood. Studies suggest that ICOS promotes antitumor effector T cell responses, while also promoting the protumor immunosuppressive functions of regulatory T cells (Tregs). To elucidate this dual role of ICOS in T cell tumor immunity, we utilized a murine model of metastatic melanoma. Initial experiments showed that *Icos* deletion in all T cells did not affect tumor burden, whereas selective *Icos* deletion in Tregs reduced the number of tumor nodules. Further analysis of the dynamics of the $CD8^+$ T cells and Treg cells in the tumor microenvironment via single-cell RNA sequencing revealed two distinct effector $CD8^+$ T cell populations expressing differential levels of genes such as T-bet and Eomes, with an increase in Eomes expression following *Icos* deletion. Consistent with this, *Icos* deletion in Treg cells, as well as in all T cells, resulted in increased frequencies of $Eomes^+$, as well as granzyme B and perforin expressing $CD8^+$ T cells at an early stage of tumor growth. To confirm our transcriptomic results, and to determine which antitumor effects driven by ICOS are intrinsic to the $CD8^+$ T cell populations as opposed to those resulting from impaired Treg cell functions, an adoptive transfer experiment using OT1 transgenic $CD8^+$ T cells was performed. Results suggest that *Icos* deletion in Tregs cells enhances $CD8^+$ T cell maturation and effector function in the tumor, whereas $CD8^+$ T cell intrinsic effects are negligible. Our work will contribute to establishing the differential requirements for ICOS in effector and regulatory T cells in cancer, which could improve the use of ICOS immunotherapy in the clinic.

Résumé

« *Inducible T-cell costimulator* » (ICOS) est un récepteur de co-stimulation exprimé par les cellules T activées qui est essentiel pour leur activation et fonction. L'expression d'ICOS est associée avec l'efficacité des inhibiteurs des points de contrôle immunitaire, et plusieurs études ciblant ICOS sont en train d'être investiguées comme traitement potentiel contre le cancer. Cependant, le rôle d'ICOS dans l'immunité antitumorale n'est pas entièrement compris. Des recherches suggèrent qu'ICOS promeut les réponses antitumorales des cellules T effectrices tout en promouvant les fonctions immunosuppressives des cellules T régulatrices (Treg). Pour élucider ce double rôle d'ICOS dans l'immunité contre le cancer, nous avons utilisé un modèle murin de mélanome métastatique. Des résultats préliminaires ont montré que la déplétion d'ICOS chez toutes les cellules T n'a pas d'influence sur la charge tumorale, tandis que la déplétion d'ICOS seulement chez les cellules Treg a réduit le nombre de nodules tumoraux. L'analyse de la dynamique des cellules T CD8 et Treg via le séquençage d'ARN unicellulaire a révélé deux populations distinctes de cellules T CD8 effectrices exprimant des niveaux différentiels de gènes tels que T-bet et Eomes, avec une augmentation de l'expression d'Eomes suivant la déplétion d'ICOS. Conformément à cela, la déplétion d'ICOS dans les cellules Treg, ainsi que dans toutes les cellules T, a augmenté la fréquence des cellules T CD8 exprimant Eomes, le granzyme B, et la perforine dans un stade précoce de croissance tumorale. Pour confirmer nos résultats transcriptomiques et pour déterminer quels effets antitumoraux induits par ICOS sont intrinsèques aux populations de cellules T CD8 ou dus à l'altération des cellules Treg, une expérience de transfert adoptif utilisant des cellules T CD8 transgéniques OT1 a été réalisée. Les résultats suggèrent que la déplétion d'ICOS dans les cellules Treg renforce la maturation et les fonctions effectrices des cellules T CD8 dans la tumeur, tandis que les effets intrinsèques de la déplétion d'ICOS dans les cellules CD8 sont négligeables. Notre travail contribuera à établir les besoins différentiels d'ICOS dans les cellules T

effectrices et Treg dans le contexte du cancer, ce qui pourrait améliorer l'utilisation d'ICOS dans la clinique comme cible thérapeutique.

Acknowledgements

I want to thank my supervisor Dr. Woong-Kyung Suh for his guidance and support throughout my degree. Thank you for taking a chance on me when I was an inexperienced undergraduate student, and for providing me with wonderful training and a welcoming lab environment. I appreciate all the advice and wisdom shared during our meetings, and I look forward to working together during my doctoral training.

I would like to thank the Suh lab members who provided great companionship during my degree. Special thanks to Joanna, Jinsam, and Antoine for the excellent training I received at bench and in bioinformatics. To the previous Suh lab members, Joanna, Jinsam, and Vincent: I appreciate all of the great advice received during our interactions, even if they were limited. To the present Suh lab members, Saba and Antoine: I appreciate your friendship and all of your help in the lab, and I look forward to working with you over the next few years.

Thank you to everyone at the IRCM core facilities who helped me with the experimentations, and a special thanks to the CPA animal technicians (Manon Laprise, Karyne Deschênes, Mariane Canuel) who accommodated all of my intravenous injection requests.

I would also like to thank the members of my advisory committee, Dr. Ciriaco Piccirillo and Dr. Christopher Rudd, for taking the time to provide me with advice on my project and on my degree in general.

A big thank you to all of my friends for their support and for encouraging me to push myself out of my comfort zone. Thank you for all the fun times and adventures, and for your companionship.

Last but not least, a huge thank you to my family, especially to my parents, for making all of this possible and encouraging me to follow my passions. You are my rock and I am eternally grateful for everything you have done, and continue to do, for me.

Contribution of Authors

All chapters in this thesis were written by Nikoletta Diamantopoulos and proofread by Dr. Woong-Kyung Suh. Results section 3.1 was written by Nikoletta Diamantopoulos based on data from Joanna Li's thesis.

The study was conceived and supervised by Dr. Woong-Kyung Suh. Experiments were designed by Nikoletta Diamantopoulos, Joanna Li, and Dr. Woong-Kyung Suh. The mice in this study were genotyped by Nikoletta Diamantopoulos, Joanna Li, Antoine Bouchard, Saba Mohammaei, Jinsam Chang, and Vincent Panneton. Intravenous injections were perfomed by animal technicians Manon Laprise, Karyne Deschênes, and Mariane Canuel at the IRCM animal facilities.

The single cell RNA sequencing experiments were performed by Joanna Li and the Molecular Biology platform at the IRCM with the advice of Vincent Panneton and Dr. Woong-Kyung Suh. Single cell RNA sequencing data was analyzed by Nikoletta Diamantopoulos with input from Joanna Li, Antoine Bouchard, and Dr. Woong-Kyung Suh. All figures in the main body of the thesis, as well as Supplemental figure 3.3, were generated by Nikoletta Diamantopoulos with advice from Dr. Woong-Kyung Suh. Supplemental figures 3.1 and 3.2, as well as their respective figure legends, were generated and written by Joanna Li, who also performed the corresponding experiments.

List of Figures

List of Abbreviations

ANOVA: analysis of variance

APC: antigen-presenting cell

ATP: adenosine 5'-triphosphate

Bcl6: B-cell lymphoma 6

CCR: CC chemokine receptor

CD : cluster of differentiation

CTL: cytotoxic T-lymphocyte

CTLA-4: cytotoxic T-lymphocyte associated protein 4

Cx3cr1: C-X3-C motif chemokine receptor 1

Cxcl: C-X-C motif ligand

CXCR: C-X-C motif chemokine receptor

DC: dendritic cell

DP: double positive

EDTA: ethylenediaminetetraaceticacid

Eomes: Eomesodermin

FasL: Fas ligand

Foxp3: forkhead box P3

GC: germinal center

GITR: glucocorticoid-induced TNFR-related protein

Gzmb: granzyme B

ICB: immune checkpoint blockade

ICOS: inducible T-cell costimulator

ICOSL: inducible T-cell costimulator ligand

IFN: interferon

Ig: immunoglobulin

IL: interleukin

ILC: innate lymphoid cell

KO : knockout

LAG-3: lymphocyte-activation gene 3

LCMV: lymphocytic choriomeningitis virus

MFI: mean fluorescence intensity

MHC: major histocompatibility complex

NK: natural killer

NKT: natural killer T

OVA: ovalbumin

PD-1: programmed cell death protein 1

PI3K: phosphoinositide 3-kinase

PLCγ1: phospholipase C gamma 1

Prf: perforin

pTreg: peripheral Treg

scRNA-seq: single-cell RNA sequencing

SP: single positive

TBK1: TANK-binding kinase 1

TCR: T cell receptor

TF: transcription factor

TGF-β: transforming growth factor beta

Th: T helper

TIL: tumor-infiltrating lymphocyte

TIM-3: T-cell immunoglobulin and mucin domain 3

TME: tumor microenvironment

TNF: tumor necrosis factor

Treg: regulatory T

Trm: tissue resident memory T cell

tTreg: thymic Treg

UMAP: uniform manifold approximation and projection

WT: wildtype

YFP: yellow fluorescent protein

Chapter 1: Introduction

1.1 T cells in cancer

1.1.1 Cancer immunoediting and the tumor microenvironment

The immune system is actively involved in controlling cancer. Both innate and adaptive arms of the immune system play a role in this process, termed immunoediting. Immunoediting is comprised of three stages: elimination, equilibrium, and escape. In the elimination phase, the immune system is able to recognize tumor cell epitopes as non-self due to the somatic mutations that are specific to transformed cancer cells[1]. The tumor cells recognized by the immune system are subsequently eliminated. In the equilibrium phase, the growing tumor is being controlled by the cells of the immune system. This exerts selection pressure on the tumor, which may eventually result in tumor cells escaping the immune attack[2]. Mechanisms of escape include downregulation of the major histocompatibility complex (MHC) class I and tumor antigens, as well as the development of an immunosuppressive tumor microenvironment (TME)[3].

The TME of solid tumors, such as that of melanoma, comprises many different cellular and soluble components that can interfere with and affect the immune response to cancer. Tumor cells, as well as vascular, stromal, and immune cells, make up the cellular compartment, whereas chemokines and cytokines are the main soluble mediators present in the TME[4]. Many of these components, such as the tumor vasculature and stromal cells, represent a physical barrier for immune cell infiltration[4]. Therefore, different tumors can have varying degrees of immune cell infiltration depending on the composition of the TME. On one hand, tumors such as those of melanoma and lung cancer are considered “hot” due to their high degree of immune infiltration, which results in higher response to immunotherapies. On the other hand, tumors such as prostate and breast cancer are considered “cold”, as they are poorly infiltrated with immune cells, and do not respond well to immunotherapies[5]. As a result, the TME and its

degree of immune cell infiltration heavily impacts the immune response to cancer. The adaptive immune system is highly involved in this response to cancer and has been extensively researched in order to develop effective immunotherapies[6]. In the following sections, the major anti and protumor cells of the adaptive immune response in cancer will be reviewed.

1.1.2 $CD8^+$ T cells

$CD8^+$ cytotoxic T-lymphocytes (CTLs) are known to be the major effector antitumor T cells. $CD8^+$ T cells originate from the bone marrow and develop and mature in the thymus. There, they gain the expression of the αβ T cell receptor (TCR), CD4, and CD8 proteins, and through their interaction with thymic epithelial cells expressing peptide-MHC class I complexes, these double positive (DP) thymocytes lose the expression of CD4 and become single-positive (SP) thymocytes expressing CD8[7]. Cells that bind peptide-MHC with intermediate affinity are positively selected for and can then exit the thymus. In the context of cancer, $CD8^+$ T cells encounter antigen presenting cells (APCs) presenting tumor antigens in the context of MHC class I in tumor-draining lymph nodes and in the tumor. Dendritic cells (DCs) are the most potent of these APCs[8]. Through their interaction with $CD103^+$ DCs, CD8+ T cells will receive TCR and CD28 stimulation[9, 10], signals necessary for T cell priming, and following their activation, will acquire their effector functions.

$CD8^+$ T cells directly target and kill tumor cells via multiple mechanisms. First, CTLs contain cytotoxic granules that are released upon T cell activation. These granules contain multiple cytotoxic proteins such as granzymes and perforin, and they act on their target cells by fusing to their plasma membrane, releasing their cytotoxic contents, and inducing cell death[11]. Granzymes B and A are the most studied and abundant granzymes, which are serine proteases that promote target cell death via multiple mechanisms such as the cleavage of caspases and gasdermin B (GSDMB)[11, 12]. Importantly, this process relies on perforin, which

is required to form a pore in the membrane of the target cell to allow granzymes to enter[13, 14]. Additionally, CTLs can mediate tumor cell killing via their FasL that binds Fas on tumor cells, which triggers apoptosis[15, 16]. Aside from these main mechanisms of direct cell killing, $CD8^+$ T cells can also produce the pro-inflammatory cytokine IFN-γ. IFN-γ is known to promote the upregulation of MHC class I on the surface of tumor cells, which in turn promotes antigen presentation and tumor cell elimination by CTLs[17]. Additionally, IFN-γ expression by $CD8^+$ T cells has also been shown to mediate effective CTL motility and cytotoxicity[18], as well as the inhibition of angiogenesis in the tumor[19].

Multiple transcription factors (TFs) are involved in the differentiation and maturation of CTLs into effector cells[20]. Two important TFs involved in this process are T-bet and Eomesodermin (Eomes). T-bet and Eomes are members of the T-box family of TFs and they have 74% sequence identity in their T-box regions[21]. T-bet, originally found to be a key TF involved in Th1 cell development[22], is also known to be essential for effector CTL differentiation. In $CD8^+$ T cells, a deficiency in T-bet was associated with reduced IFN-γ expression and cytotoxic capacity in antigen-specific OT-I cells following *in vitro* stimulation[23], and mice deficient for T-bet showed impaired formation of short-lived effector cells in a model of LCMV infection[24]. Furthermore, Eomes was originally described in *Xenopus* as being essential for embryogenesis[25, 26], and was later found to be expressed in the mammalian immune system[21]. Overexpression of Eomes in $CD8^+$ T cells *in vitro* was sufficient to induce the expression of IFN-γ, granzyme B, and perforin independent of T-bet, and the absence of Eomes impaired the cytotoxic capacity of T cells[21]. Further investigation of the role of T-bet and Eomes in CTLs determined that T-bet induces IFN-γ and granzyme B expression, whereas Eomes drives that of IFN-γ and perforin[27]. Interestingly, T-bet and Eomes appear to have redundant functions in CTLs, with T-bet being essential for the early induction of effector cells expressing IFN-γ, and late Eomes expression inducing IFN-γ and perforin[27, 28]. Consistent

with this, concurrent knockout of T-bet and Eomes resulted in impaired cytotoxic capacity and inefficient clearance of viral infection[29]. Therefore, both T-bet and Eomes are important for CTL differentiation and cytotoxic function.

In the context of chronic infection, such as chronic viral infection or cancer, constant antigenic stimulation promotes a state of $CD8^+$ T cell exhaustion. Following the peak of T cell expansion, exhaustion is favored over memory cell formation, which is characterized by the expression of multiple co-inhibitory receptors and by the loss of effector functions[30]. These receptors include PD-1, CTLA-4, LAG3, and TIM-3 among others, and they function to dampen T cell activation. Interestingly, T-bet and Eomes may also play a role in the exhaustion process[31], with studies in viral infection showing that T-bet^{hi} cells giving rise to more terminally exhausted $Eomes^{hi}$ cells[32]. Therefore, T-bet and Eomes may also be key TFs in the differentiation of CTLs in the TME.

Given the importance of CTLs in antitumor immunity, many immunotherapies targeting $CD8^+$ T cells have been developed such as immune checkpoint blockade (ICB). ICB targets co-inhibitory receptors expressed on CTLs that are induced by chronic antigenic stimulation, and in doing so, prevent the inhibition of antitumor CTL responses[33]. ICB blocking antibodies against PD-1 and CTLA-4 are currently being used in clinic, and multiple others are being tested in clinical trials in order to harness the potent antitumor functions of CTLs[34].

1.1.3 $CD4^+$ T helper cells

Another subset of T cells highly involved in the immune response to cancer are $CD4^+$ T helper cells. These conventional $CD4^+$ T cells develop in the thymus alongside their $CD8^+$ counterparts, however, they differ in that they recognize antigen presented by APCs in the context of MHC class II. Once they exit the thymus and encounter their cognate antigen, $CD4^+$ T cells will differentiate into different T helper (Th) cell lineages based on cytokines received

from their activating APCs as well as key transcription factors induced by these cytokines[35]. In cancer, $CD4^+$ T helper cells have two main functions: promoting $CD8^+$ T cell responses, and directly exerting antitumor functions. Indirectly, $CD4^+$ Th cells can promote antitumor immunity by interacting with DCs via CD40-CD40L ligation, which enhances the expression of MHC-I and co-stimulatory receptors such as CD80, CD86, and CD70 on DCs[36, 37, 38]. Consequently, DCs are better able to activate CTLs, with studies showing that $CD4^+$ T cell help enhances cytotoxicity and migration, and downregulates inhibitory receptors[36, 39, 40]. Furthermore, $CD4^+$ T cells can directly promote antitumor immunity. Notably, Th1 cells, which are characterized by the expression of T-bet, have been shown to prevent cancer progression through the production of the cytokines IFN-γ and TNFα[41]. Additionally, these cells have also been implicated in the recruitment of antitumor natural killer (NK) cells and macrophages to the tumor[35].

1.1.4 Regulatory T cells

In contrast to the antitumor functions of conventional $CD4^+$ Th cells, $CD4^+$ regulatory T cells (Treg cells) are the major protumor T cell subset in cancer. These cells are characterized by their master transcription factor Foxp3 and are essential in maintaining self-tolerance, with mutations in Foxp3 in both humans and rodents resulting in severe autoimmunity[42, 43]. Treg cells can either arise from the thymus (tTreg) or the periphery (pTreg). In the thymus, upon interaction with peptide-MHC class II, some $CD4^+$ thymocytes with strong TCR signal strength escape negative selection and upregulate CD25, which enhances IL-2 signaling and promotes Foxp3 induction[44]. In the periphery, strong TCR signal strength and TGF-β can induce Foxp3 expression in naïve $CD4^+$ T cells[45].

In cancer, Treg cells are attracted to the tumor by chemokines, and this is mediated by the expression of chemokine receptors, such as CCR4 and CXCR3, on Treg cells[46].The

generation of pTreg cells in the tumor has also been described, where integrin αvβ8 expressed on tumor cells can interact with latent TGF-β on T cells to promote Treg cell differentiation[47]. As a result, Treg cells can make up a significant portion of $CD4^+$ T cells in the tumor, which is associated with worse prognosis in multiple cancers due to their immunosuppressive functions[48].

Treg cells promote immunosuppression in the tumor via multiple mechanisms. First, CTLA-4 on Treg cells can bind to CD80 and CD86 on APCs with higher affinity than CD28, which can dampen T cell activation[49]. CTLA-4 binding to CD80/86 can also result in the removal and degradation of these co-stimulatory receptors by the Treg cells[50]. Additionally, since Treg cells express CD25 (IL2Ra) and do not produce the IL-2 that they require, they can deprive effector T cells of IL-2 and prevent their activation in the TME[46]. Another key mechanism of suppression is through the secretion of immunosuppressive cytokines such as IL-10 and TGF-β, as well as the cytotoxic proteins granzyme B and perforin[46, 51]. In addition, it has been shown that the expression of CD39 and CD73 on Treg cells can metabolize ATP into adenosine, which inhibits effector T cell function[52].

1.2 ICOS

1.2.1 Structure, expression pattern, and signaling

Originally discovered in 1999, inducible T-cell costimulator (ICOS) is a member of the CD28 family of co-stimulatory receptors[53]. ICOS is a homodimer and is composed of an extracellular Ig domain, a type I transmembrane glycoprotein segment, and a cytoplasmic tail[54]. Unlike CD28, ICOS is expressed in an inducible manner following TCR ligation, and ICOS ligation with its ligand ICOSL is highly regulated to prevent overactivation, a process that is mediated by the internalization of ICOS and the shedding of ICOSL[55]. ICOS is expressed predominantly in activated T cell subsets, but is also known to be expressed in other immune cells such as NK cells and γδ T cells[54]. ICOS is also expressed constitutively by a subset of

Treg cells[56] as well as ILCs[57]. Furthermore, ICOSL, a member of the B7 family of ligands, is expressed by APCs. However, unlike CD80 (B7.1) and CD86 (B7.2), ICOSL has also been found to be expressed by other cell types such as ILCs, alveolar epithelial cells, and muscle cells[57, 58, 59].

ICOS signaling is mediated by three signaling pathways through motifs in its cytoplasmic tail[54]. First, ICOS-ICOSL ligation can trigger PI3K signaling via the TYR181 residue in the YMFM SH2-binding motif[60]. Additionally, ICOS can also induce intracellular Ca^{2+} flux, which is mediated by PLCγ1 and relies on the KKKY motif[61]. Finally, ICOS has also been shown to promote TBK1 signaling in T follicular helper (Tfh) cells, and this is mediated by the IProx signaling motif[62].

1.2.2 ICOS function in T cells

In T cells, ICOS co-stimulation enhances T cell activation and promotes T cell proliferation, survival, and cytokine production[54]. Multiple studies have investigated the role of ICOS in various T cell subsets. One of the most studied subsets with respect to ICOS is the T follicular helper (Tfh) cell population. Tfh cells are essential for humoral immunity, as they provide help to B cells in germinal centers (GCs) to promote antibody production. ICOS has been shown to play an essential role in Tfh cell biology, with a loss of ICOS resulting in a dramatic reduction in the Tfh population at steady-state and post-immunization[60]. This is due to the requirement for ICOS in the expression of Bcl6, the master transcription factor for Tfh cells[63]. As a result, ICOS is also required for the recruitment of Tfh cells to GCs and for the interaction of Tfh cells with B cells within the GCs[54]. In addition to the role of ICOS in humoral immunity, its role in other T cell subsets, such as those involved in antitumor immunity, has also been investigated and will be reviewed in the following sections.

1.2.2.1 ICOS in $CD8^+$ T cells

The role of ICOS in $CD8^+$ T cells is not well studied and remains poorly understood. An early study using a sarcoma tumor model showed that only tumors expressing ICOSL were rejected, and that this was dependent on $CD8^+$ T cells[64]. ICOSL expression by tumor cells was also shown to promote tumor-specific CTL cytotoxicity, with $ICOSL^+$ tumor cells being targeted by CTLs more effectively than $ICOSL^-$ tumor cells[65]. Furthermore, another study found that ICOS-deficient mice were less able to control Salmonella infection compared to wildtype (WT) mice[66]. This was associated with a reduction in antigen-specific $CD8^+$ T cells in the spleen, as well as a reduction in IFN-γ^+ $CD8^+$ T cells. ICOS deficient $CD8^+$ T cells also exhibited lower cytotoxic potential *in vitro* compared to their WT counterparts[66]. These data suggest that ICOS-deficient $CD8^+$ T cells could be defective in their effector function.

ICOS has also recently been shown to be important for the effective generation of $CD8^+$ tissue resident memory (Trm) cells. ICOS-deficient $CD8^+$ T cells were unable to form Trm cells compared to their ICOS sufficient counterparts when transferred into WT mice infected with LCMV[67]. Seeing as Trm cells are present in tumors and are increasingly thought to have antitumor functions[68], ICOS could also be contributing to antitumor immunity by supporting Trm cell generation.

1.2.2.2 ICOS in $CD4^+$ Th1 cells

Contrary to $CD8^+$ T cells, the role of ICOS has been studied more extensively in $CD4^+$ T cells. However, the role of ICOS in Th1 cells differs based on the infection model used[69]. In *Mycobacterium tuberculosis* and in *Chlamydia muridarum* infections, ICOS-deficient and ICOSL-deficient mice had an enhanced Th1 response, as seen by the increase in IFNγ production[70, 71]. Similarly, IFNγ was increased in mice receiving anti-ICOS neutralizing antibody in a model of *Schistosoma mansoni* infection[72]. However, in other infection models,

ICOS appears to support Th1 responses. In *Salmonella enterica* and *Listeria monocytogenes* infection models, disruption of ICOS signaling through ICOS deficiency or through administration of an ICOS-Ig fusion protein resulted in a reduction in IFNγ production by $CD4^+$ T cells[66, 73]. This suggests that ICOS is required for optimal Th1 responses. However, it is difficult to determine the true Th1-intrinsic defect that arises from the inhibition of ICOS signaling in these models, as other T cell subsets such as Treg cells are also impacted[69].

1.2.2.3 ICOS in Treg cells

Multiple studies have investigated the role of ICOS in Treg cells. Approximately 20% of Treg cells are $ICOS^+$, and ICOS has been shown to be involved in Treg generation, survival, proliferation, and suppressive function[74]. Mice with a deficiency in ICOS co-stimulation show reduced peripheral Treg cell numbers, which was due to a reduction in Treg cell survival rather than a defect in thymic output[75]. This is likely due to the instability and downregulation of Foxp3 due to reduced Foxp3 expression[76]. Furthermore, $ICOS^+$ Treg cells have superior proliferative capacity than their $ICOS^-$ counterparts[77, 78], suggesting that ICOS also regulates Treg cell proliferation. Additionally, ICOS is also involved in Treg suppressive functions, although the mechanism is poorly understood. In some early studies, $ICOS^+$ Treg cells were shown to have increased production of IL-10[79, 80]. However, it appears that ICOS signaling is not mainly responsible for IL-10 production, as mice with a IL-10 deficiency developed more severe disease than mice with an ICOS deficiency[74]. In addition, mice lacking ICOS selectively in Treg cells were able to control the incidence of autoimmunity at steady state, and ICOS-deficient Treg cells did not have impaired suppressive capacity[81]. However, loss of ICOS in Treg cells in a model of atopic dermatitis showed increased inflammation[81], suggesting that $ICOS^+$ Treg cells have an important role in inflammatory settings.

1.3 ICOS in cancer

1.3.1 ICOS as a biomarker for immunotherapeutic response

In cancer, ICOS was initially seen as a biomarker for response to immune checkpoint blockade (ICB) therapy. In bladder cancer, patients being treated with anti-CTLA-4 had elevated tumor antigen-specific $ICOS^+CD4^+$ T cells in peripheral blood and in the tumor, which resulted in an increased effector-to-Treg cell ratio[82]. Similar results were also seen in breast cancer and lung cancer patients, where anti-CTLA-4 therapy promoted an increase in both peripheral $CD4^+$ and $CD8^+$ T cells expressing ICOS[83, 84]. Furthermore, ICOS expression on T cells has also been associated with a beneficial response to ICB. $ICOS^+$ $CD4^+$ T cells in melanoma and bladder cancer patients treated with anti-CTLA-4 were found to be a biomarker for response[85, 86] and recently, a similar association was found in lung cancer patients treated with PD-1 blockade[87].

1.3.2 ICOS in antitumor immunity

Given that ICOSL can be expressed in the tumor, it can provide a key signal for $ICOS^+$ tumor infiltrating T cell subsets that are involved in anti and protumor immunity. $ICOS^+$ T cells being enriched in patients undergoing ICB treatment is one piece of evidence suggesting a major antitumor role for ICOS in the TME. Additionally, animal studies have also investigated its role in antitumor immunity. In the CTL and Th1 compartments, anti-CTLA-4 administered to WT mice bearing B16/BL6 melanoma tumors resulted in increased $CD8^+$ T and $CD4^+$ T cells, similar to that found in humans[88]. An increase in the $ICOS^+CD8^+$ and $ICOS^+CD4^+$ T cell-to-Treg cell ratio was also observed, and $ICOS^+$ T cells produced more IFN-γ than $ICOS^-$ CTLs when stimulated with tumor antigen[88]. Additionally, another study found that granzyme B expression by CTLs was significantly increased in mice receiving anti-CTLA-4 in combination with a tumor cell vaccine expressing ICOSL, and this was associated with reduced tumor

burden[89]. These mice also displayed an increased frequency of IFN-γ^+TNFα^+ CD4$^+$ effector T cells. Collectively, these data suggest that ICOS expression in CTLs and Th1 cells promotes antitumor immunity.

1.3.3 ICOS in protumor immunity

On the other hand, ICOS expression in Treg cells can promote tumor growth, which supports a protumor role for ICOS in the TME. ICOSL has been found to be expressed in tumor cells such as in human melanoma, which could potentiate the function of Treg cells through ICOS co-stimulation. In human melanoma, the expression of ICOSL by tumor cells was shown to promote the expression of CD25, Foxp3, and IL-10 by Treg cells[90]. Additionally, acute myeloid leukemia cells were also found to express ICOSL, which promoted the induction of IL-10$^+$ Treg cells and resulted in reduced survival[91]. Furthermore, ICOSL expression by dendritic cells in tumors has also been shown to promote ICOS$^+$ Treg cell accumulation in ovarian cancer, which was associated with reduced survival[92], and similar observations were also seen in human breast cancer[93]. Therefore, ICOS co-stimulation could result in sustained Treg cells in the TME, which promotes immunosuppression and tumor growth.

1.4 Rationale and objectives of the research

ICOS has important functions in T cell subsets involved in tumor immunity (**Figure 1.1**). ICOS expression on effector T cells appears to promote antitumor immunity, whereas its expression on Treg cells can promote tumor growth. Despite this, not much is known about the role of ICOS in CTLs, which are the main antitumor T cells. Furthermore, ICOS agonist or antagonist antibodies are being tested in the clinic as an immunotherapy for cancer[94], but results are not impressive. In addition, it remains unclear whether ICOS plays a mostly antitumor or

protumor role in cancer. Thus, the role of ICOS in cancer-immune interactions needs to be better understood in order to improve the use of ICOS immunotherapy in the clinic.

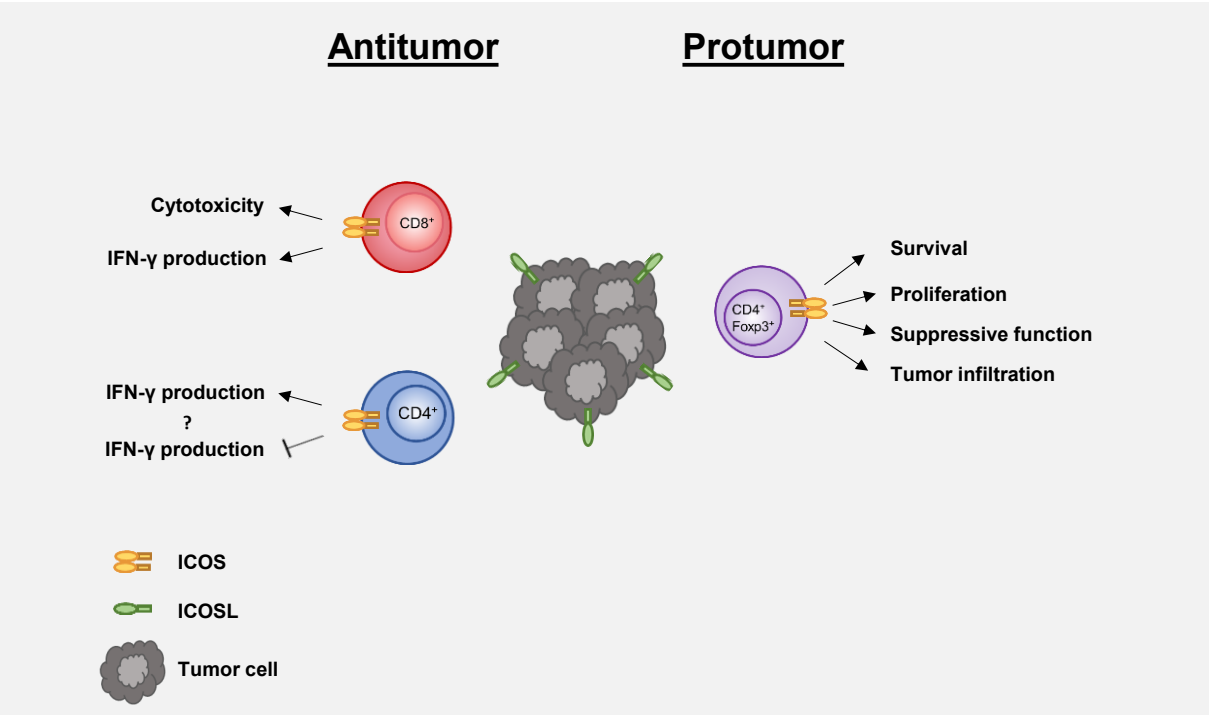

Figure 1.1 The role of ICOS in anti and protumor T cell subsets. ICOS is expressed in both antitumor and protumor T cell subsets. ICOS costimulation in effector $CD8^+$ T cells can promote their cytotoxic function, as well as the production of IFNγ. In effector $CD4^+$ T cells, ICOS costimulation has been shown to either enhance or inhibit the production of IFN-γ depending on the infection model used. Evidence also suggests that ICOS promotes survival, proliferation, suppressive function, and tumor infiltration of $Foxp3^+$ Treg cells. Given that ICOSL is expressed by tumor cells, ICOS may play a dual role in the tumor microenvironment via the support of both pro and antitumor T cell subsets.

Therefore, we hypothesize that ICOS co-stimulation has a dual role in anti and protumor T cell responses by modulating Treg cells and effector $CD8^+$ T cells. Our objectives are the following:

1. To assess the role of ICOS in T cell subsets on tumor growth.
2. To profile tumor-infiltrating $CD8^+$ T cells and Treg cells from tumor-bearing mice lacking ICOS in all T cells or selectively in Treg cells.
3. To determine the $CD8^+$ T cell-intrinsic and Treg cell-mediated effects of *Icos* deletion in antitumor immunity.

Chapter 2: Materials and Methods

2.1 Mice

The Foxp3$^{YFP\text{-}cre}$ (Jax 016959) and CD4^{cre} (Jax 017336) mice used in this study were acquired from the Jackson Laboratory, and ICOS conditional knockout mouse lines were generated as previously described[95]. Male Foxp3$^{YFP\text{-}cre}$ mice were used for Foxp3cre lines, and females were used for CD4cre lines to allow for co-housing prior to experimentation. Six-to-thirteen-week-old mice were used for experiments. All mice were housed and bred under specific pathogen-free conditions in the Institut de Recherches Cliniques de Montréal animal facility, and all experiments were performed in accordance with animal use protocols approved by the Institut de Recherches Cliniques de Montréal Animal Care Committee. For intravenous injection of B16-OVA melanoma cells, each mouse was injected in the tail vein with 6 x 10^5 cells in 200 µL of sterile PBS.

2.2 Tissue culture

The B16-ovalbumin (B16-OVA) melanoma cell line was obtained from Dr. John Stagg, Université de Montréal, and were stored in liquid nitrogen until use[96]. B16-OVA cells were cultured in Dulbecco's modified Eagle's medium (DMEM) supplemented with 4.5 g/L D-glucose, 2 mM L-glutamine, 1 mM sodium pyruvate, 10 % heat-inactivated fetal bovine serum (all from Wisent), as well as with 10 mM HEPES, 100 U/mL penicillin, 100 ug/mL streptomycin, and 55 µM 2-mercaptoethanol (all from ThermoFisher). T-175 cell culture flasks for adherent cells (Sarstedt) were used to culture the cells. Trypsin-EDTA (0.05 %, ThermoFisher) was used to passage cells every 2-3 days. Cells were harvested for injection after the 2nd or 3rd passage using 10 mM EDTA (ThermoFisher) in PBS, and a final concentration of 3 x 10^6 cells/mL was prepared.

2.3 Flow cytometry

Lungs were perfused with cold PBS using a 25G needle and, following extraction, the tumor-bearing lungs were cut into pieces using scissors. 10 mL of collagenase solution containing 300 U/mL collagenase type II (Worthington Biochemical) and 10 mg/mL DNAse I (MilliporeSigma) was added to each lung and digested for 50 minutes at 37 °C with 300 rpm horizontal shaking. Lung digests were then filtered through 40 μM cell strainers, and red blood cells were depleted. Cells were filtered once more through 70 μM cell strainers and 1/3 of the cells (1 x 10^6 cells) were kept for staining. To distinguish between viable and dead cells, cells were stained in 100 uL volume with fixable viability dye (eFluor 450 or APC-eFluor780, ThermoFisher) for 15 minutes at 4 °C. To block non-specific binding, 1 μg of anti-CD16/32 (BioXCell) was added to each sample for 5 minutes at room temperature. Surface staining was performed in staining buffer containing 1 % bovine serum albumin (Wisent) in PBS and at 4 °C for 20 minutes. Intracellular staining was performed by fixing and permeabilizing cells for 45 minutes at 4 °C using the Foxp3 Transcription Factor Fixation/Permeabilization Concentrate and Diluent set (ThermoFisher). Cells were then stained for 45 minutes at 4 °C in 1X Permeabilization buffer (ThermoFisher). The following antibodies were used for flow cytometry: anti-CD45 FITC (30-F11, Invitrogen), anti-CD45.1 FITC (A20, Invitrogen), anti-CD45.2 Brilliant Violet 785 (104, BioLegend), anti-CD4 BUV395 (GK1.5, BD Biosciences), anti-CD8 PerCP-Cyanine5.5 (53-6.7, Invitrogen), anti-CD44 Brilliant Violet 605 (IM7, BD Biosciences), anti-PD-1 Brilliant Violet 421 (J43, BD Biosciences), anti-Eomes PE-Cyanine7 (Dan11mag, Invitrogen), anti-T-bet Brilliant Violet 711 (4B10, BioLegend), anti-Granzyme B APC (QA18A28, BioLegend), anti-Perforin PE (S16009A, BioLegend), anti-Foxp3 Alexa Fluor 700 (FJK-16s, Invitrogen). In addition, the following antibodies were used for the day 10 analysis in the CD4cre model: anti-CD44 PE (IM7, BD Pharmingen), anti-TIM-3 Brilliant

Violet 650 (RMT3-23, BioLegend), anti-Ly108 APC (330-AJ, BioLegend), anti-PD-1 PE-Cyanine7 (J43, Invitrogen). Data were acquired on LSRFortessa (BD Biosciences) and analyzed using FlowJo version 10 (BD Biosciences).

2.4 Single-cell RNA sequencing and analysis

One control (*Cd4*^{cre}*Icos*$^{+/+}$ or *Foxp3*^{cre}*Icos*$^{+/+}$) and one knockout (*Cd4*^{cre}*Icos*$^{f/f}$ or *Foxp3*^{cre}*Icos*$^{f/f}$*)* mouse were injected intravenously with B16-OVA cells. 10 days later, the lungs were collected and processed, and tumor-infiltrating T cells were stained with viability dye, anti-CD45, anti-CD4, anti-CD8 and anti-CD44. For the Foxp3$^{YFP\text{-}cre}$ mice, live CD8$^+$ T cells (CD45$^+$CD8$^+$CD44$^+$), non-Treg CD4$^+$ T cells (CD45$^+$CD4$^+$CD44$^+$), and Treg cells (CD45$^+$CD4$^+$YFP$^+$) were sorted. For the CD4^{cre} mice, live CD8$^+$ T cells (CD45$^+$CD8$^+$CD44$^+$) and CD4$^+$ T cells (CD45$^+$CD4$^+$CD44$^+$) were sorted. All sorting was performed using the BD FACSAria (BD Biosciences). We used 16 500 cells (CD4cre) and 32 500 cells (Foxp3cre) from control and knockout mice for library preparation. Libraries were generated at the Institut de Recherches Cliniques de Montréal Molecular Biology and Functional Genomics Core facility using the following components from 10x Genomics: Chromium Next GEM Chip G Single Cell kit, Chromium Next GEM Single Cell 3' GEM, Library & Gel Bead kit v3.1, Chromium i7 Multiplex kit. Sequencing was performed by Genome Québec using a NovaSeq 6000 (Illumina).

Analysis of the single-cell RNA sequencing data was carried out using Seurat v3.0[97]. For the single cell expression matrix analysis, cells with more than 10 % mitochondrial RNA contamination, corresponding to dead cells, were filtered out of the dataset. Cells with less than 200 and more than 6000 unique genes expressed were also eliminated, as they correspond to empty droplets and multiplets. The data was then log normalized, and following the identification of the most differentially expressed genes within the samples, the data was

scaled. Linear dimensional reduction was subsequently performed using the Principal Component Analysis (PCA) approach based on the 2000 most variable features. The first 40 most important components produced by the PCA analysis were selected, and a Shared Nearest Neighbour (SNN) graph was constructed. Modularity Optimizer version 1.3.0[98] was used to identify 19 clusters in the CD4cre dataset, and 20 clusters in the Foxp3cre dataset. The Uniform Manifold Approximation and Projection (UMAP) method was used to visualize the cells on a two-dimensional space[99]. T cell clusters were identified and separately clustered, generating 13 clusters in the Foxp3cre dataset and 15 clusters in the CD4cre dataset. For the analysis of $CD8^+$ T cells, clusters corresponding to $CD8^+$ T cells were identified based on *Cd8a* expression and separately clustered, generating 6 clusters in both Foxp3cre and CD4cre datasets. For the analysis of Treg cells in the Foxp3cre dataset, $CD4^+$ T cells were identified based on *Foxp3* expression and separately clustered, generating 10 clusters. Analysis of gene expression patterns were then performed using the Seurat functions FeaturePlot, DoHeatmap, and VlnPlot.

2.5 Adoptive transfer

Nine male CD45.1 mice were injected intravenously with 6 x 10^5 B16-OVA cells. 5 days post-challenge, spleens from one male *OT1*$^+$*Icos*$^{+/-}$ and one male *OT1*$^+$*Icos*$^{-/-}$ mouse were collected. Single cell suspensions of splenocytes were obtained via mechanical disruption through 70 uM filters in PBS, and red blood cells were subsequently eliminated. $CD8^+$ T cells were then isolated using the EasySep Mouse $CD8^+$ T Cell Isolation Kit (StemCell), and cells were prepared to a final concentration of 5 x 10^6 cells/mL. Mice in experimental groups intravenously received 1 x 10^6 OT1 T cells in 200 µL PBS, and the control group received 200µL PBS. Mice were euthanized and tumor-infiltrating lymphocytes were analyzed 17 days post-tumor cell injection.

2.6 Statistical analysis

To assess statistical significance, two-tailed Student *t* tests were used for single comparisons, and one-way ANOVA with pairwise comparisons was used for comparisons between three groups. The Wilcoxon rank sum test executed by the Seurat FindMarkers function was used for comparisons of single cell gene expression between experimental groups in each cluster. *p* values were used to judge statistical significance as follows: ns = $p > 0.05$, *$p < 0.05$, **$p < 0.01$, ***$p < 0.001$, ****$p < 0.0001$. Prism 9 (GraphPad software) was used for analysis.

Chapter 3: Results

3.1 Tumor burden is decreased following the deletion of *Icos* gene in Treg cells

To assess the role of ICOS in different T cell subsets in tumor immunity, we utilized a metastatic model of murine melanoma in which melanoma cells injected into the tail vein of mice circulate and form metastatic nodules in the lung. In this way, we can measure tumor burden via the number of tumor nodules in the lung, as well as analyze the intratumoral T cells via flow cytometry. To assess the effect of *Icos* deletion in Treg cells in our model, we intravenously injected B16-OVA melanoma cells (B16 melanoma cells expressing the chicken ovalbumin antigen) into control mice ($Foxp3^{cre}Icos^{+/+}$) and mice lacking *Icos* selectively in Treg cells ($Foxp3^{cre}Icos^{f/f}$). In this system, *Icos* is deleted in Treg cells while remaining intact in all other T cell subsets. Tumor burden and intratumoral T cells were then analyzed 17 days following tumor cell injection (**Supp. Figure 3.1A**). Day 17 corresponds to a late stage of tumor growth in this model, and therefore, can be informative as to the overall effect of *Icos* deletion on tumor burden. Compared to the control group, tumor burden was reduced in the $Foxp3^{cre}Icos^{f/f}$ mice (**Supp. Figure 3.1B**). Flow cytometry analysis revealed a reduction in the frequency and numbers of total $CD4^+$ T cells, as well as the numbers of $CD8^+$ T cells (**Supp. Figure 3.1C and D)**. $CD8^+$ T cell frequencies were trending towards a reduction, but this was not significant (**Supp. Figure 3.1D**). Interestingly, $Foxp3^+CD4^+$ Treg cells were more drastically decreased compared to effector cells in the $Foxp3^{cre}Icos^{f/f}$ mice (**Supp. Figure 3.1E and F**), which resulted in enhanced effector $CD4^+$ to Treg and $CD8^+$-to-Treg ratios (**Supp. Figure 3.1H**). In addition, $Foxp3^{cre}Icos^{f/f}$ mice showed decreased percentages of $CD44^+$ activated Treg cells, whereas the mean fluorescence intensity (MFI) of Foxp3 was unaffected (**Supp. Figure 3.1G**). Overall, these data suggest that $Foxp3^+$ Treg cells are impaired in $Foxp3^{cre}Icos^{f/f}$ mice, which could be enhancing the antitumor effector T cell compartment and resulting in the reduction of tumor nodules observed.

In contrast, deleting *Icos* in all $CD4^+$ and $CD8^+$ T cells, including Treg cells, did not affect the tumor burden at day 17 post-tumor challenge, as there was no significant difference in tumor nodule number between $Cd4^{cre}Icos^{+/+}$ control mice and $Cd4^{cre}Icos^{f/f}$ knockout mice (**Supp. Figure 3.2A**). Infiltrating T cell analysis showed no differences in the percentage and numbers of total $CD4^+$ and $CD8^+$ T cells **(Supp. Figure 3.2B and C**), as well as those of Treg cells and effector $CD4^+$ T cells (**Supp. Figure 3.2D and E**) between genotypes. As a result, the effector $CD4^+$-to-Treg and $CD8^+$-to-Treg ratios were unchanged (**Supp. Figure 3.2F**). Together with our Foxp3cre data in which Treg cells are affected by *Icos* deletion, our CD4cre results suggest that when all T cells are deficient for *Icos*, the functions of multiple T cell subsets could be impaired, which results in no overall difference in tumor burden.

3.2 Single-cell RNA transcriptome analysis reveals two populations of effector T cells in metastatic tumor-bearing lungs

Since we observed differences in the Treg cell population at day 17 post-tumor injection in the Foxp3cre model, we next sought to understand the changes occurring in individual T cell compartments in more detail by performing single-cell RNA sequencing (scRNAseq) experiments using tumor infiltrating T cells. This would give insight into the way that Treg cells are affected by *Icos* deletion, and how this impacts other T cell subsets involved in the tumor immune response. In addition, since day 17 represents a late stage of tumor growth in this model, we decided to analyze T cells from the lungs of tumor-bearing mice at day 10 post-challenge in order to capture the dynamic stage of tumor growth. To this effect, $Foxp3^{cre}Icos^{+/+}$ and $Foxp3^{cre}Icos^{f/f}$ mice were challenged with tumor cells, and intratumoral T cells were obtained and sequenced 10 days following injection (**Figure 3.1A**). Live tumor-infiltrating $CD44^+CD8^+$ T cells, $CD44^+CD4^+Foxp3^-$ T cells, and $CD4^+Foxp3^+$ Treg cells (based on Foxp3-YFP reporter) were sorted from the lungs of one $Foxp3^{cre}Icos^{+/+}$ and one $Foxp3^{cre}Icos^{f/f}$ mouse,

mixed at a 1:1:1 ratio, and scRNA-seq was performed using 10x Genomics platform. UMAP projections following downstream analysis of the sequenced cells revealed 13 clusters (**Figure 3.1B**). With the exception of the minuscule cluster 12 appearing only in the *Foxp3*^{cre}*Icos*$^{f/f}$ mouse, there are no unique clusters associated with each genotype. Furthermore, CD8$^+$ T cells, Treg cells, and effector CD4$^+$ T cells were grouped into distinct clusters, as seen via the expression of *CD8a*, *Cd4*, and *Foxp3* (**Figure 3.1B and C**). As expected, most clusters corresponded to activated T cells, as determined by the expression of *Cd44,* with some clusters also expressing *Sell* (CD62L), which is a marker of naïve and memory cells. As a result, the CD8$^+$ and non-Treg CD4$^+$ T cell clusters are CD44$^+$, whereas Treg cell clusters 0, 4, and 6 are *Cd44*$^-$*Sell*$^+$, *Cd44*$^+$*Sell*$^+$, and *Cd44*$^+$*Sell*$^-$, respectively (**Figure 3.1B and C**).

To further analyze the CD8$^+$ T cell compartment, all CD8$^+$ T cell clusters were isolated and re-clustered. UMAP projections revealed 6 distinct clusters, with no unique clusters appearing between the genotypes (**Figure 3.1D**). Overall, cluster 2 is decreased, and clusters 1 and 4 are enriched, in the *Foxp3*^{cre}*Icos*$^{f/f}$ mouse (**Figure 3.1E**). Further analysis of gene expression patterns showed that clusters 1 and 2 correspond to activated effector CD8$^+$ T cells, as seen by their *Cd44*$^+$*Sell*$^-$ phenotype (**Figure 3.1F**), as well as the expression of effector genes such as granzyme B (*Gzmb*), perforin (*Prf1*), IFN-γ (*Ifng*), Fas ligand (*Fasl*), and *Cx3cr1* (**Figure 3.1G**). Therefore, two predominant populations of activated effector CD8$^+$ T cells are present in this tumor microenvironment.

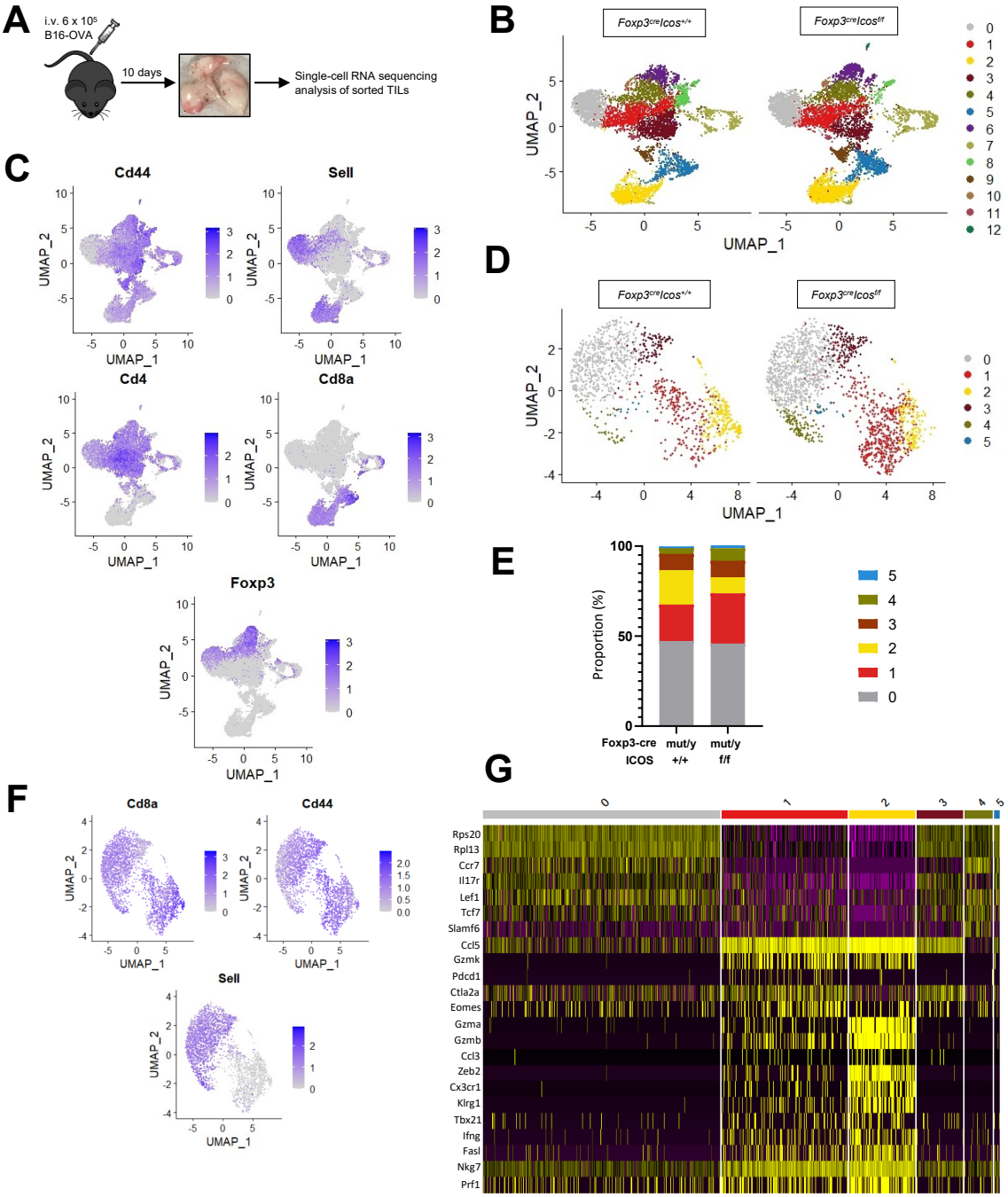

Figure 3.1 Two activated effector CD8$^+$ T cell populations are present in the lungs of tumor-bearing Foxp3cre mice. (A) Experimental setup for murine metastatic melanoma model. (B-G) Single-cell RNA sequencing analysis of sorted tumor-infiltrating T cells from one *Foxp3*$^{YFP\text{-}cre}$*Icos*$^{+/+}$ (abbreviated as *Foxp3*^{cre}*Icos*$^{+/+}$) and one *Foxp3*$^{YFP\text{-}cre}$*Icos*$^{f/f}$ (abbreviated as *Foxp3*^{cre}*Icos*$^{f/f}$) mouse 10 days post-challenge with B16-OVA melanoma cells as in (A). (B) UMAP projections of T cell clusters in *Foxp3*^{cre}*Icos*$^{+/+}$ and *Foxp3*^{cre}*Icos*$^{f/f}$ mice. (C) Feature plots of *Cd44*, *Sell*, *Cd4, Cd8a*, *Foxp3* expression. (D) UMAP projections of CD8$^+$ T cell clusters in *Foxp3*^{cre}*Icos*$^{+/+}$ and *Foxp3*^{cre}*Icos*$^{f/f}$ mice. (E) Proportions of CD8$^+$ T cell clusters. (F) Feature plots of *Cd8a, Cd44, Sell* expression. (G) Heatmap of CD8$^+$ T cell cluster markers.

3.3 *Icos* gene deletion in Treg cells differentially regulates the Eomes^{hi} and T-bet^{hi} effector CD8^{+} tumor-infiltrating T cell populations

To further understand how *Icos* deletion in Treg cells impacts these two activated tumor-infiltrating CD8^{+} T cell populations, we compared the expression of key effector genes between genotypes for both clusters. Of the two populations, cluster 2 had the highest expression level of effector genes (**Figure 3.2A and B**). Interestingly, when comparing between the control (*Foxp3^{cre}Icos$^{+/+}$*) and knockout (*Foxp3^{cre}Icos$^{f/f}$*) samples, there was a decrease in the expression levels of the key CTL effector genes *Prf1*, *Ifng*, and *Cx3cr1* in the knockout, whereas *Gzmb* expression was lower but not significantly so (**Figure 3.2B**). In addition, gene expression analysis from Figure 3.1G identified the transcription factor T-bet (*Tbx21*) as a marker for cluster 2 (**Figure 3.2E**), further reinforcing the notion that this population is composed of effector CTLs. Consistent with the effector gene analysis, T-bet was also downregulated in the knockout sample **(Figure 3.2D**). Taken together with the cluster proportion data from Figure 3.1E where the T-bet^{hi} cluster 2 is decreased in the knockout mouse, these results suggest that T-bet^{+} effector cell function is dampened when Treg cells lose *Icos*.

On the other hand, PD-1 (*Pdcd1*) was identified as a prominent marker for cluster 1 (**Figure 3.1G**). Similarly, other co-inhibitory receptors such as LAG3 (*Lag3*) and CTLA4 (*Ctla4*) were also expressed predominantly by cluster 2 (**Figure 3.2C**), and comparing control and knockout samples showed that the expression of PD-1 and LAG3 was increased in the knockout sample (**Figure 3.2D**). These co-inhibitory receptors are commonly seen as markers of exhausted and dysfunctional T cells at later stages of tumor growth, however, they can also be considered as activation markers, as their expression is induced following antigen stimulation. Consistent with this, Ly108 (*Slamf6*), a gene known to be expressed by precursor

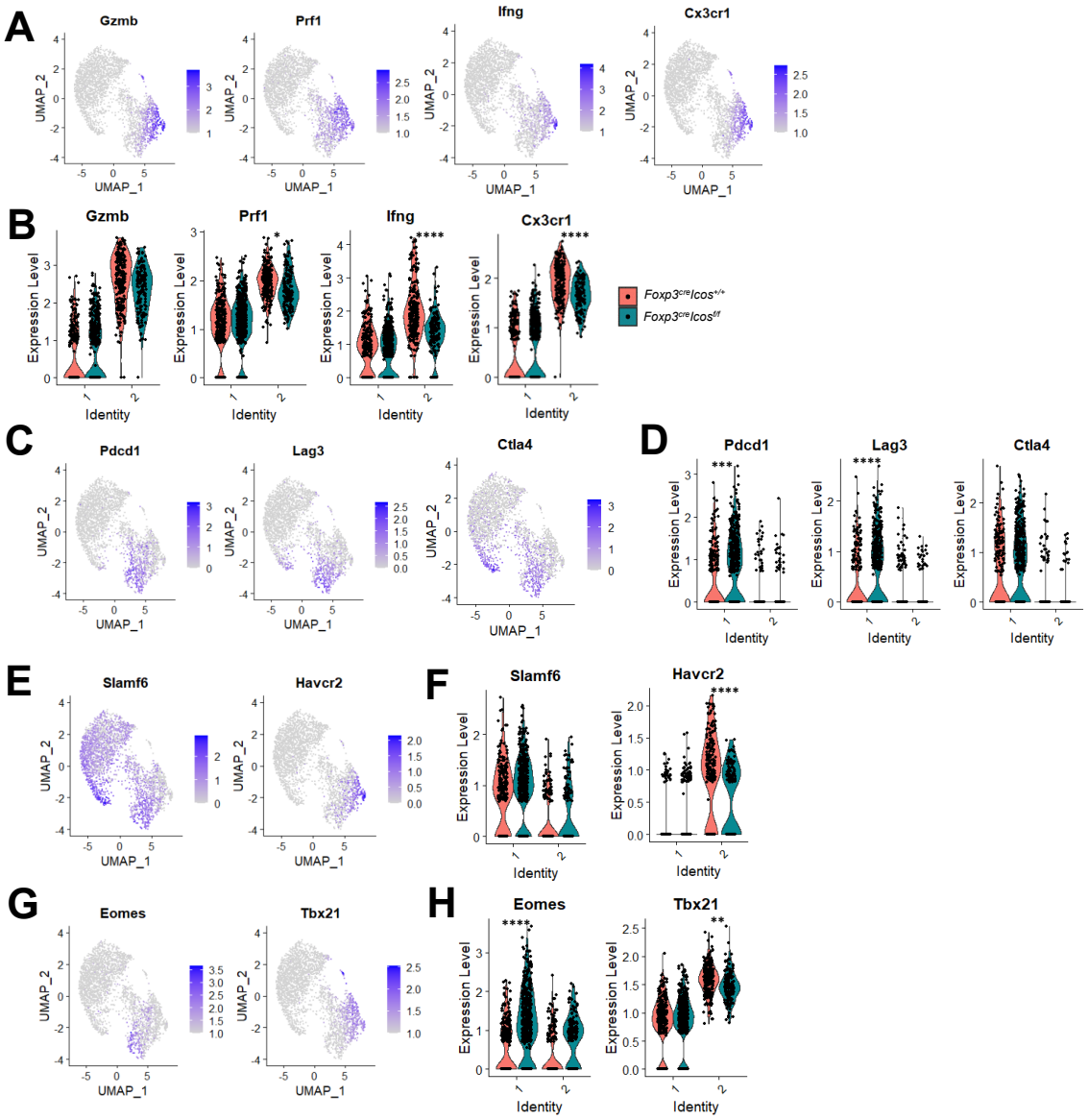

Figure 3.2 Eomes is upregulated in the Eomes^{hi} population when *Icos* is lost in Treg cells. Single-cell RNA sequencing data of sorted tumor-infiltrating T cells from one *Foxp3^{cre}Icos$^{+/+}$* and one *Foxp3^{cre}Icos$^{f/f}$* mouse 10 days post-challenge with B16-OVA melanoma cells. (A) Feature plots *of Gzmb, Prf1, Ifng, Cx3cr1* expression. (B) Violin plots of *Gzmb, Prf1, Ifng, Cx3cr1* expression in clusters 1 and 2 as defined in Figure 3.1D. (C) Feature plots of *Pdcd1, Lag3, Ctla4* expression. (D) Violin plots *of Pdcd1, Lag3, Ctla4* expression in clusters 1 and 2. (E) Feature plots of *Slamf6* (Ly108) and *Havcr2* (TIM-3) expression. (F) Violin plots of *Slamf6* (Ly108) and *Havcr2* (TIM-3) expression in clusters 1 and 2. (G) Feature plots of *Eomes and Tbx21* (T-bet) expression. (H) Violin plots of *Eomes and Tbx21* expression in clusters 1 and 2. Each dot corresponds to one cell. *p<0.05, **p<0.01, ***p<0.001, ****p<0.0001.

to exhausted cells, was also expressed by cluster 2, whereas TIM-3 (*Havcr2*), a co-inhibitory receptor known as a marker for late-stage exhaustion, was not expressed by these cells (**Figure 3.2E**). Rather, cluster 2 expressed TIM-3, and this expression was decreased in the knockout

(**Figure 3.2F**). This suggests that cells in cluster 2 may represent CTLs undergoing maturation as opposed to exhaustion.

Furthermore, gene expression analysis identified the transcription factor Eomes as a marker for cluster 1 (**Figure 3.1G and Figure 3.2G**). Interestingly, *Eomes* expression was significantly unregulated in the knockout mouse (**Figure 3.2H**). These results are also consistent with the cluster proportion data from Figure 3.1E where cluster 1 is expanded in the knockout sample, suggesting that activated antigen-experienced effector $CD8^+$ T cells expressing Eomes are expanded when Treg cells lose ICOS.

3.4 *Icos* gene deletion in all T cells recapitulates some phenotypes observed in the Treg-specific deletion model

Since our transcriptomic data suggest that a Treg-specific *Icos* deletion significantly affects the effector $CD8^+$ T cell compartment, and that these changes ultimately contributed to the decreased tumor burden observed in Supp. Figure 3.2B, we next sought to determine if a loss of *Icos* in all T cells would give similar results. This would also provide insight into any effector $CD8^+$ T cell-intrinsic changes mediated by the deletion of *Icos*. To do so, we performed another round of single-cell RNA sequencing using the CD4cre model, where one $Cd4^{cre}Icos^{+/+}$ control mouse and one $Cd4^{cre}Icos^{f/f}$ knockout mouse were challenged with tumor cells. Since this mouse line does not contain a reporter for Foxp3, Treg cells were not able to be directly sorted. To compensate for this, and to ensure that we obtained a significant number of Treg cells for analysis, $CD44^+CD4^+$ T cells and $CD44^+CD8^+$ T cells were sorted from the lungs of tumor-bearing mice at day 10 post-tumor cell injection and mixed at a 2:1 ratio prior to sequencing. UMAP projections following downstream analysis of tumor-infiltrating T cells revealed 15 clusters, with no unique clusters appearing or disappearing in the knockout sample (**Figure 3.3A**). As expected from our sorting strategy, all T cells expressed *Cd44*, with some

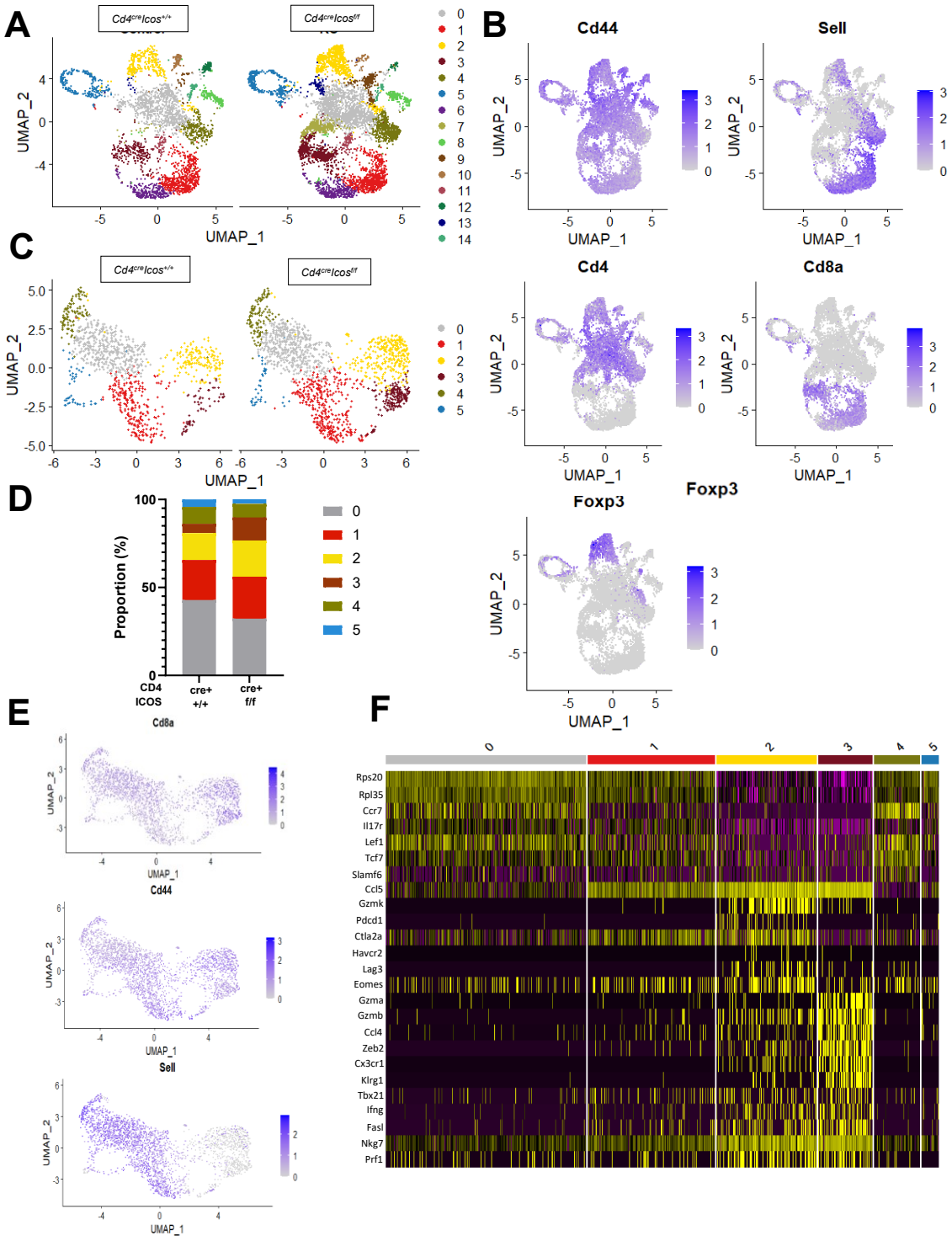

Figure 3.3 Two activated effector CD8$^+$ T cell populations are present in the lungs of tumor-bearing CD4cre mice. Single-cell RNA sequencing analysis of sorted CD44$^+$ tumor-infiltrating T cells from one *Cd4^{cre}Icos$^{+/+}$* and one *Cd4^{cre}Icos$^{f/f}$* mouse 10 days post-challenge with B16-OVA melanoma cells as in Figure 3.1A. (A) UMAP projections of T cell clusters in *Cd4^{cre}Icos$^{+/+}$* and *Cd4^{cre}Icos$^{f/f}$* mice. (B) Feature plots of *Cd44*, *Sell*, *Cd4, Cd8a*, *Foxp3*. (C) UMAP projections of CD8$^+$ T cell clusters in *Cd4^{cre}Icos$^{+/+}$* and *Cd4^{cre}Icos$^{f/f}$* mice. (D) Proportions of CD8$^+$ T cell clusters. (E) Feature plots of *Cd8a, Cd44, Sell*. (F) Heatmap of CD8$^+$ T cell cluster markers.

coexpressing *Sell* (CD62L) (**Figure 3.3B**). Clusters 1, 3, and 6 represent CD8$^+$ T cells, cluster

5 corresponds to $CD4^+$ and $CD8^+$ proliferating T cells, and all other clusters are comprised of $CD4^+$ T cells (**Figure 3.3A and B**). Treg cells were present in the dataset and correspond to cluster 2 based on *Foxp3* expression (**Figure 3.3B**).

Further clustering of solely $CD8^+$ T cells resulted in 6 clusters, with no unique clusters appearing or disappearing in the knockout (**Figure 3.3C**). Similar to our Foxp3cre dataset, all clusters were $Cd44^+$, with two (clusters 2 and 3) showing a $Cd44^+Sell^-$ phenotype (**Figure 3.3E**). However, unlike in the Foxp3cre dataset, both activated effector clusters were enriched in the knockout sample (**Figure 3.3D**). Additionally, key genes expressed by these two populations include effector genes encoding Granzyme B, Perforin, Cx3cr1, Klrg1, and Nkg7 (**Figure 3.3F**). Therefore, both of the $Cd44^+Sell^-$ populations correspond to activated effector $CD8^+$ T cells and are present in both our Foxp3cre and CD4cre mouse models.

Furthermore, comparing the expression of genes in both clusters showed that cluster 3 expressed higher levels of effector genes, including *Gzmb*, Perforin (*Prf1)*, *Ifng*, and *Cx3cr1* (**Figure 3.4A**). This is similar to the data from our Foxp3cre model. However, when comparing the expression of these genes between control and knockout samples for these clusters, we found that, of the effector genes analyzed, only *Cx3cr1* was upregulated in cluster 3 of the knockout sample, whereas *Gzmb, Prf1*, and *Ifng* were not significantly altered (**Figure 3.4B**). T-bet was once again the dominantly expressed transcription factor in this population (**Figure 3.4G**), however, its expression was unchanged in the knockout sample (**Figure 3.4H**).

Performing a similar analysis on cluster 2, we found that, similar to the Foxp3cre dataset, cluster 2 showed higher expression of inhibitory receptors such as PD-1 (*Pdcd1*), LAG3 (*Lag3*), and CTLA4 (*Ctla4*) (**Figure 3.4C**). However, while *Lag3* was upregulated, *Pdcd1* expression was lower in the knockout and *Ctla4* remained unchanged (**Figure 3.4D**). This cluster also expressed TIM-3 (*Havcr2*), while also expressing Ly108 (*Slamf6*), suggesting

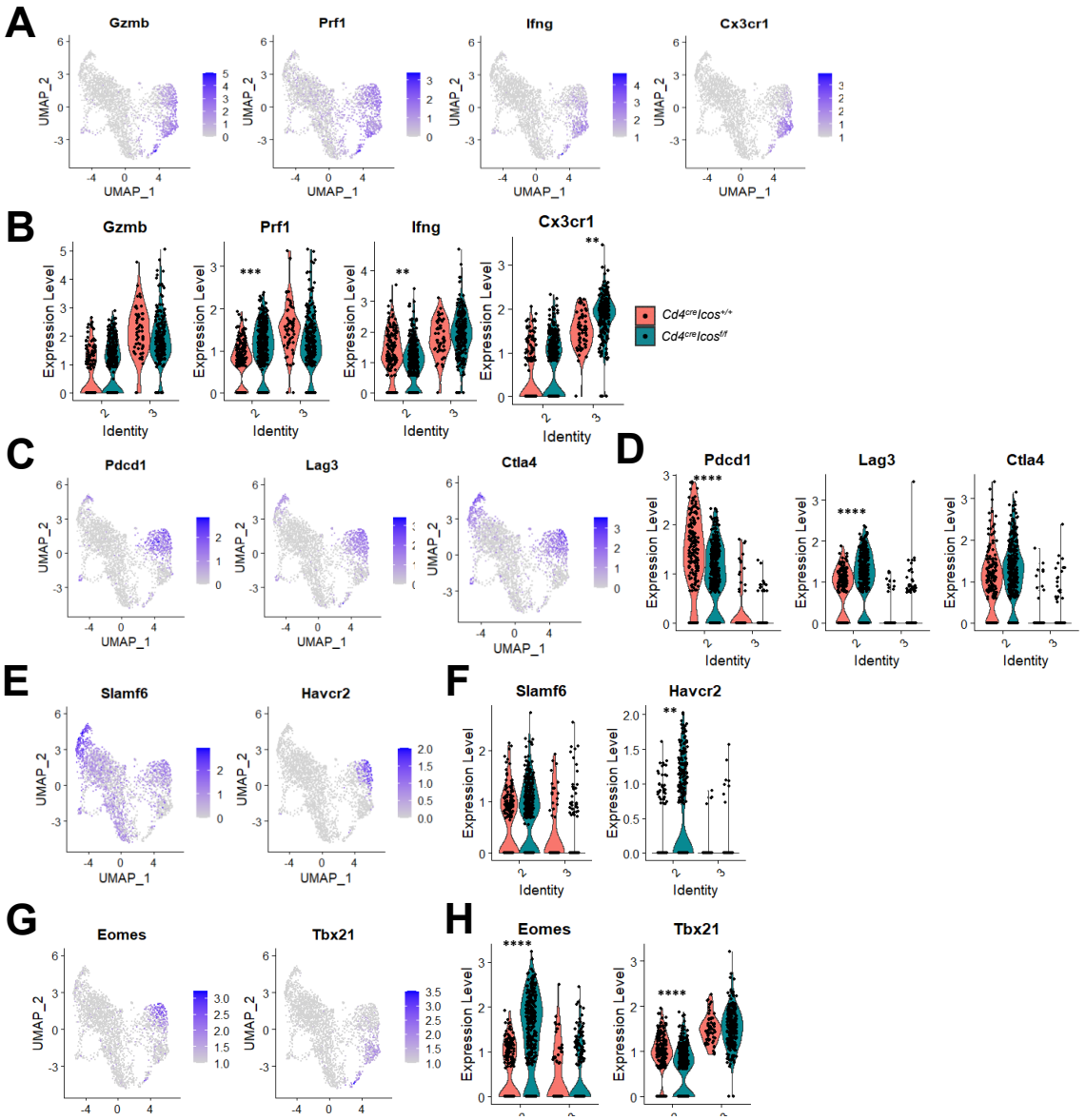

Figure 3.4 Eomes is upregulated in the Eomes^{hi} population when *Icos* is lost in all T cells. Single-cell RNA sequencing data of sorted tumor-infiltrating T cells from one *Cd4^{cre}Icos$^{+/+}$* and one *Cd4^{cre}Icos$^{f/f}$* mouse 10 days post-challenge with B16-OVA melanoma cells. (A) Feature plots *of Gzmb, Prf1, Ifng, Cx3cr1* expression. (B) Violin plots of *Gzmb, Prf1, Ifng, Cx3cr1* expression in clusters 2 and 3 as defined in Figure 3.3C. (C) Feature plots of *Pdcd1, Lag3, Ctla4* expression. (D) Violin plots *of Pdcd1, Lag3, Ctla4* expression in clusters 2 and 3. (E) Feature plots of *Slamf6* (Ly108) and *Havcr2* (TIM-3) expression. (F) Violin plots *of Slamf6*, and *Havcr2* expression in clusters 2 and 3. (G) Feature plots of *Eomes and Tbx21* (T-bet) expression. (H) Violin plots of *Eomes and Tbx21* expression in clusters 2 and 3. Each dot corresponds to one cell. **p<0.01, ***p<0.001, ****p<0.0001.

that this cluster is not exhausted (**Figure 3.4E**). Interestingly, the expression levels of *Havcr2*, as well as the effector genes *Prf1* and *Ifng* were elevated in the knockout sample for cluster 2, whereas *Slamf6* expression was unchanged (**Figure 3.4B and F**). In addition, consistent with

our previous data, *Eomes* was preferentially expressed by cluster 2 (**Figure 3.4G**), and its expression was significantly elevated in the knockout (**Figure 3.4H**). Overall, even though our transcriptomic datasets differ in certain aspects, our results from the CD4cre model confirm that two effector populations are present in the lungs of our tumor model, and that the Eomes^{hi} population is enriched when T cells lose *Icos*, which is most likely due to a loss of *Icos* in Treg cells. Additionally, these data suggest that *Icos* deletion in CD8$^+$ T cells also has an effect on their functionality. However, further studies need to be done to elucidate how ICOS costimulation is intrinsically involved in CD8$^+$ T cell function.

3.5 *Icos* gene deletion in Treg cells promotes an enhanced cytotoxic phenotype and the expansion of Eomes$^+$CD8$^+$ T cells

Since we observed clear differences in effector CD8$^+$ T cell populations at the transcriptomic level when *Icos* was absent in Treg cells, we next sought to confirm these differences at the protein level by flow cytometry. To this effect, control mice (*Foxp3^{cre}Icos$^{+/+}$*) and mice lacking *Icos* selectively in Treg cells (*Foxp3^{cre}Icos$^{f/f}$*) were challenged with B16-OVA cells, and TILs were analyzed 10 days later. To analyze intratumoral lymphocytes via flow cytometry, we gated on CD45$^+$CD4$^+$ and CD45$^+$CD8$^+$ live cells (**Supp. Figure 3.3A**). Similar to the day 17 results, there were no differences in the frequencies of total CD4$^+$ and CD8$^+$ T cells (**Figure 3.5A and B**), and there was a significant decrease in Treg cell frequency in the knockout (**Figure 3.5C and D**). However, there was no difference in the percentage of CD44$^+$ Treg cells (**Figure 3.5D**). Furthermore, to properly distinguish between tumor-specific and bystander T cells, we gated on CD44^{hi} and PD-1$^+$ CD8$^+$ T cells for further analysis (**Supp. Figure 3.3A**). At a broad population level, there were no differences in activated CD44^{hi} CD8$^+$ or in CD44^{hi}PD-1$^+$ CD8$^+$ T cells (**Figure 3.5E**).

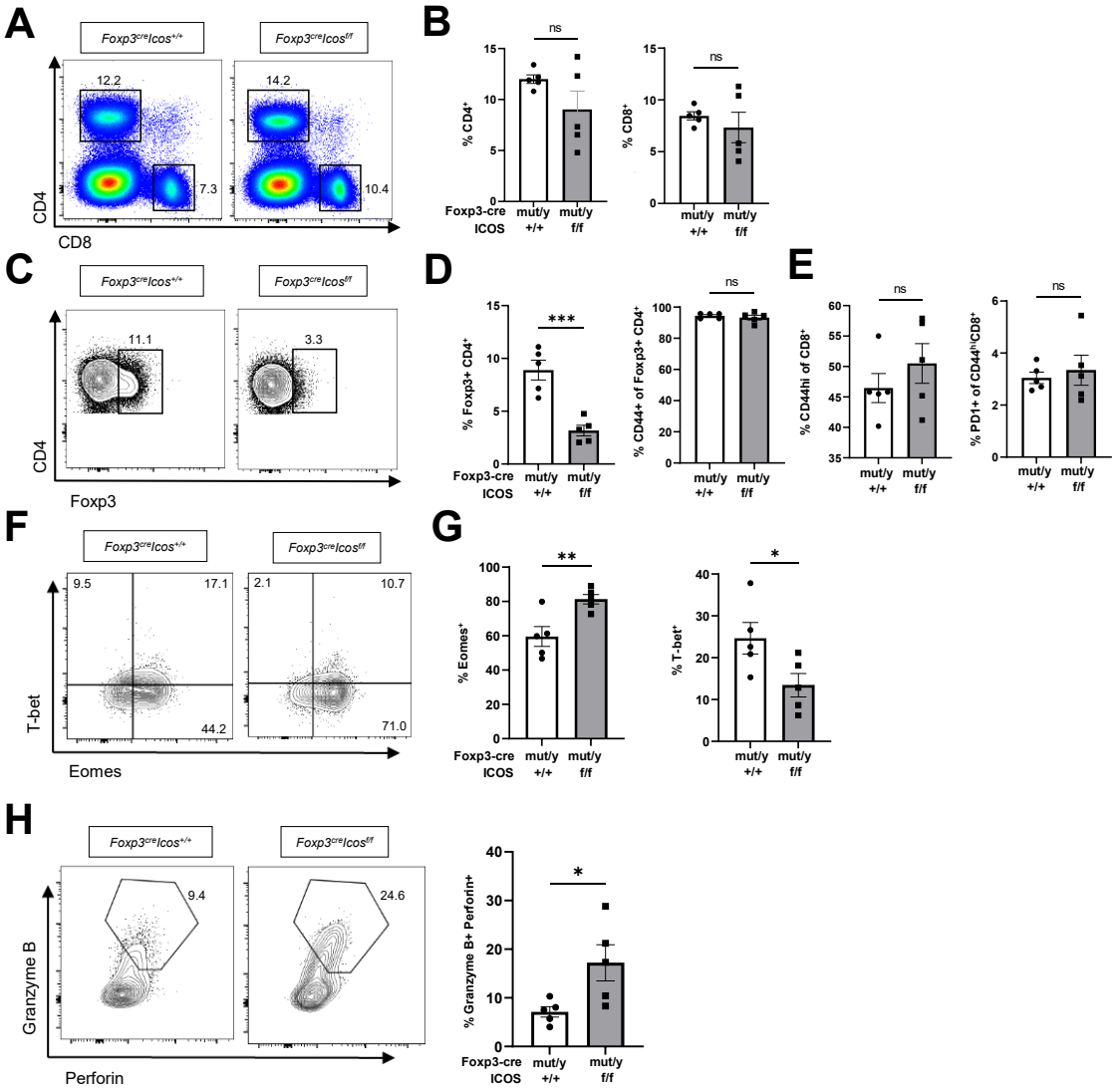

Figure 3.5 Treg-specific deletion of *Icos* promotes Eomes upregulation and cytotoxic function in CD8$^+$ T cells. 8- to 10- weeks old *Foxp3^{cre}Icos$^{+/+}$* and *Foxp3^{cre}Icos$^{f/f}$* mice were challenged with B16-OVA cells as in Figure 3.1A (n=5 each). (A-H) Flow cytometry analysis of tumor-infiltrating T cells. (A) Representative flow cytometry plots of total CD4$^+$ and CD8$^+$ T cells pre-gated on CD45$^+$ leukocytes. (B) Percentage of total CD4$^+$ and CD8$^+$ T cells. (C) Representative flow cytometry plots of Foxp3$^+$ Tregs pre-gated on total CD4$^+$ T cells. (D) Percentages of Foxp3$^+$CD4$^+$ Treg cells and CD44$^+$Foxp3$^+$CD4+ activated Tregs. (E) Percentages of CD44^{hi}CD8$^+$ activated T cells and PD-1$^+$ tumor-reactive CD8$^+$ T cells pre-gated on CD44^{hi} cells. (F) Representative flow cytometry plots of Eomes$^+$ and T-bet$^+$ CD8$^+$ T cells pre-gated on CD44^{hi}PD-1$^+$ cells. (G) Percentages of Eomes$^+$ and T-bet$^+$ CD8$^+$ T cells. (H) Representative flow cytometry plots and percentages of Granzyme B$^+$Perforin$^+$ CD8$^+$ T cells pre-gated on CD44^{hi}PD-1$^+$ cells. Data presented as mean ± SEM, ns= not statistically significant, *p<0.05, **p<0.01, ***p<0.001.

Furthermore, since we found an increase in the Eomes expressing population, as well as a decrease in the T-bet expressing population in our transcriptomic data, we analyzed the expression of Eomes and T-bet at the protein level (**Supp. Figure 3.3B**). Consistent with our

single-cell data, the percentage of $CD44^{hi}PD\text{-}1^{+}$ $CD8^{+}$ T cells expressing Eomes was significantly elevated in the *Foxp3*^{cre}*Icos*$^{f/f}$ mice and that of $CD44^{hi}PD\text{-}1^{+}$ $CD8^{+}$ T cells expressing T-bet was decreased (**Figure 3.5F and G**). Concomitantly, the frequency of $CD44^{hi}PD\text{-}1^{+}$ $CD8^{+}$ T cells coexpressing granzyme B and perforin ($Gzmb^{+}Prf1^{+}$) was also significantly increased in the knockout (**Figure 3.5H**). Therefore, *Icos* deletion in Treg cells results in enhanced $Eomes^{+}$ and $Gzmb^{+}Prf1^{+}$ $CD8^{+}$ T cells in the lungs of metastatic tumor-bearing mice. This suggests that ICOS-expressing Treg cells function to prevent the maturation and function of CTLs in the tumor microenvironment.

3.6 The increase in Eomes expression in tumor antigen-specific $CD8^{+}$ T cells is not due to an intrinsic defect in ICOS costimulation

Since we observed an increase in $Eomes^{+}$ CTLs when Tregs and all T cells lose *Icos*, we next sought to determine the relative contributions of a $CD8^{+}$ T cell-intrinsic defect vs. a Treg-mediated effect. To do this, we performed an adoptive transfer experiment where OT1 T cells ($CD8^{+}$ T cells with an OVA-specific transgenic TCR) either sufficient (*Icos*$^{+/-}$) or deficient (*Icos*$^{-/-}$) for *Icos* were adoptively transferred into congenic WT mice five days following tumor cell injection. TILs were then analyzed at day 17, which corresponds to 12 days post-transfer (**Figure 3.6A**). An additional PBS control group was included to assess the impact of adoptively transferred OT1 cells on tumor burden. As expected, mice receiving OT1 cells had fewer tumor nodules compared to the PBS control. However, there was no significant difference in nodule number between the groups receiving ICOS-Het or ICOS-KO OT1 cells (**Figure 3.6B**). This suggests that *Icos*-deficient CD8+ T cells may not be severely functionally impaired.

Furthermore, to analyze the TILs, recipient and donor $CD8^{+}$ cells were distinguished based on the expression of the congenic markers CD45.1 and CD45.2, respectively (**Figure**

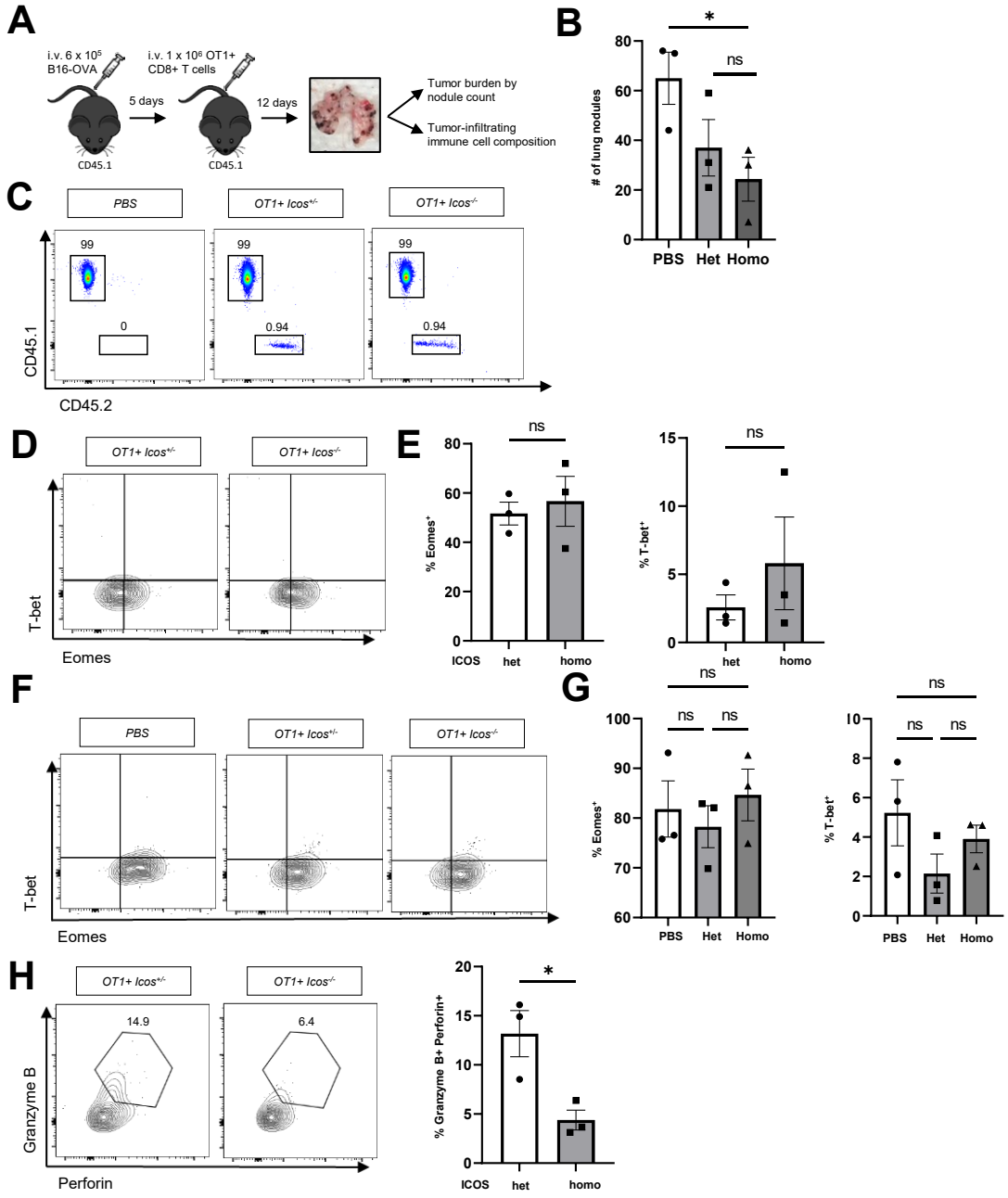

Figure 3.6 Loss of *Icos* impairs tumor antigen-specific CD8$^+$ T cell function without affecting Eomes expression. (A) Experimental setup for adoptive transfer in the murine metastatic melanoma model. 12-weeks old CD45.1 mice were challenged with B16-OVA melanoma cells, followed by *Icos*$^{+/-}$ OT1 cells, *Icos*$^{-/-}$ OT1 cells, or PBS alone (n=3 each). (B) Tumor nodule number analysis. (C) Representative flow cytometry plots of CD45.1$^+$ recipient cells and CD45.2$^+$ OT1 donor cells pre-gated on CD45$^+$CD8$^+$ T cells. (D) Representative flow cytometry plots of Eomes$^+$ and T-bet$^+$ OT1 cells. (E) Percentages of Eomes$^+$ and T-bet$^+$ OT1 cells. (F) Representative flow cytometry plots of Eomes$^+$ and T-bet$^+$ cells pre-gated on CD44^{hi}PD-1$^+$ recipient cells. (G) Percentages of Eomes$^+$ and T-bet$^+$ recipient cells. (H) Representative flow cytometry plots and percentages of Granzyme B$^+$Perforin$^+$ OT1 cells. Data presented as mean ± SEM, ns= not statistically significant, *p<0.05.

3.6C). We first analyzed Eomes and T-bet expression in OT1 cells. Unlike in our

transcriptomic data and our Foxp3cre model, there were no significant differences in the percentage of Eomes$^+$ or T-bet$^+$ populations in ICOS-Het mice compared to ICOS-KO mice (**Figure 3.6D and E**), which suggests that this effect is Treg-mediated rather than CD8$^+$ T cell-intrinsic. There was also no difference in the percentage of Eomes and T-bet expressing cells in the recipient CD44^{hi}PD-1$^+$CD8$^+$ T cell population for all three experimental groups (**Figure 3.6 F and G**). This validates that the monoclonal OT1 cells reflect the polyclonal recipient CD8$^+$ T cell population. Interestingly, there was a significant reduction in the percentage of Gzmb$^+$Prf$^+$ ICOS-KO OT1 cells compared to the ICOS-Het OT1 cells (**Figure 3.6E**). This suggests that ICOS deficiency in tumor antigen-specific CD8$^+$ T cells impacts T cell function to some extent, although this was not enough to impact overall tumor burden in our model.

3.7 CD8$^+$ T cell-intrinsic defects due to *Icos* deletion are negligible when all T cells lack *Icos*

Since we observed a significant reduction in Gzmb$^+$Prf$^+$ cells in our adoptive transfer model, which was the opposite of what we observed in the polyclonal population in our Foxp3cre model at the protein level, we next examined whether this CD8$^+$ T cell-intrinsic defect was dominant over the Treg-mediated effect of *Icos* deletion. To do this, we used the CD4cre model where *Cd4^{cre}Icos$^{+/+}$* and *Cd4^{cre}Icos$^{f/f}$* mice were challenged with tumor cells, and tumor-infiltrating T cells were analyzed 10 days later. Overall, there were no differences in the total CD4$^+$ and CD8$^+$ T cell populations, nor in the total CD44^{hi} CD8$^+$ T cells between genotypes (**Figure 3.7A and B**). However, the percentage of PD-1$^+$CD44^{hi} CD8$^+$ T cells was elevated in the knockout mice (**Figure 3.7B**). Furthermore, the frequency of Eomes$^+$ cells was also significantly increased in the *Cd4^{cre}Icos$^{f/f}$* mice, whereas that of T-bet$^+$ cells did not differ between genotypes (**Figure 3.7C and D**). Accordingly, the percentage of Gzmb$^+$Prf$^+$ cells was trending towards an increase in the knockout; however, this was not significant (**Figure 3.7E**).

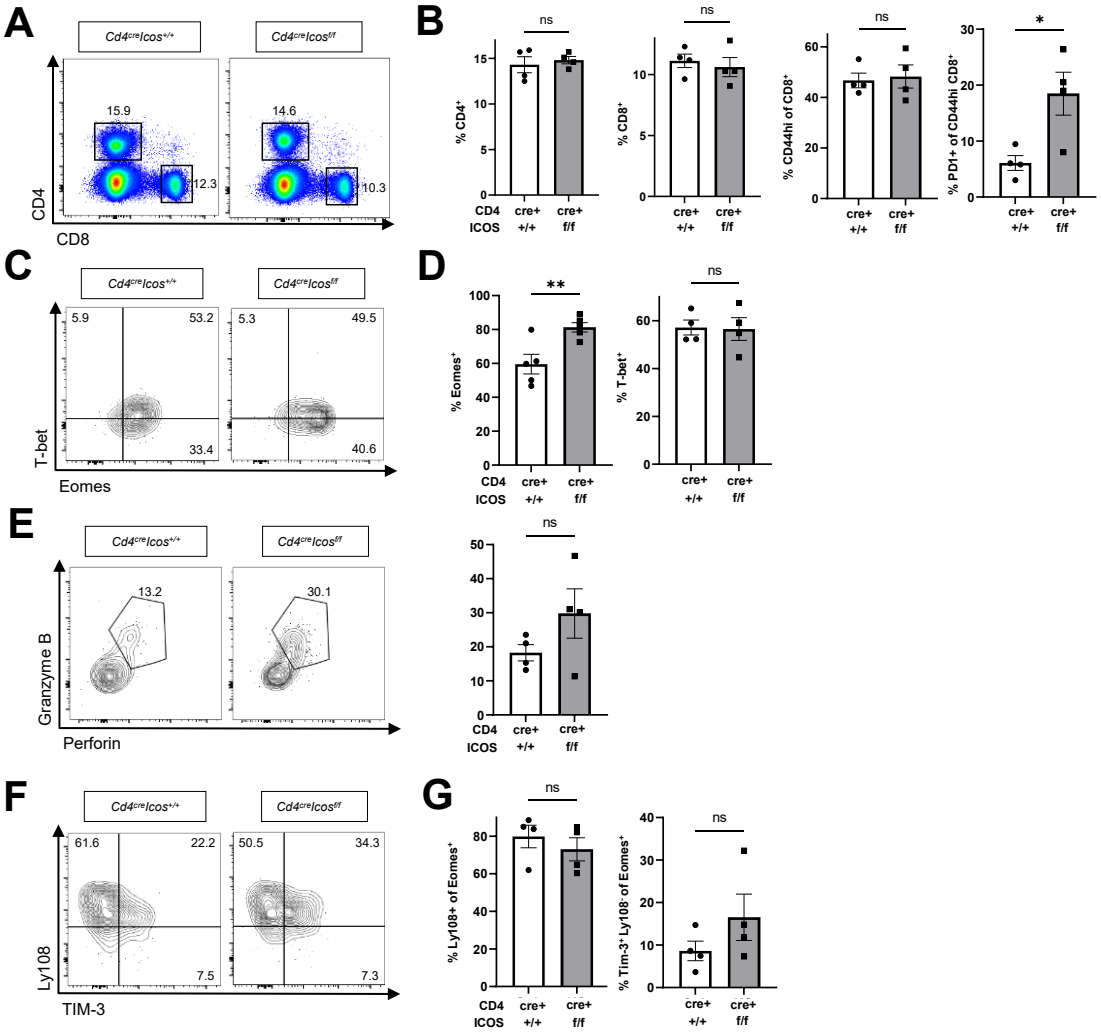

Figure 3.7 T cell-specific deletion of *Icos* promotes Eomes upregulation and cytotoxic function in CD8$^+$ T cells. 10- to 13-weeks old female *Cd4^{cre}Icos$^{+/+}$* and one *Cd4^{cre}Icos$^{f/f}$* mice were challenged with B16-OVA melanoma cells as in Figure 3.1A (n=4 each). (A) Representative flow cytometry plots of total CD4$^+$ and CD8$^+$ T cells pre-gated on CD45$^+$ leukocytes. (B) Percentages of total CD4$^+$ T cells, CD8$^+$ T cells, CD44^{hi} activated CD8$^+$ T cells, and PD-1$^+$ tumor-reactive CD8$^+$ T cells pre-gated on CD44^{hi} cells. (C) Representative flow cytometry plots of Eomes$^+$ and T-bet$^+$ CD8$^+$ T cells pre-gated on CD44^{hi}PD-1$^+$ cells. (D) Percentages of Eomes$^+$ and T-bet$^+$ CD8$^+$ T cells. (E) Representative flow cytometry plots and percentages of Granzyme B$^+$Perforin$^+$ CD8$^+$ T cells pre-gated on CD44^{hi}PD-1$^+$ cells. (F) Representative flow cytometry plots of Ly108$^+$ and TIM-3$^+$ cells pre-gated on CD44^{hi}PD-1$^+$Eomes$^+$ cells. (G) Percentages of of Ly108$^+$ and TIM-3$^+$Ly108$^-$ cells. Data presented as mean ± SEM, ns= not statistically significant, *p<0.05, **p<0.01.

This suggests that the Treg-mediated effect of *Icos* deletion in all T cells is dominant over the CD8$^+$ T cell-intrinsic defect observed in the adoptive transfer model, and that this results in an increase in Eomes expression and cytotoxic function when *Icos* is deleted. Additionally, when analyzing the Eomes$^+$ population, we found that most cells were Ly108$^+$ (**Figure 3.7F and G**),

which is consistent with our transcriptomic data. In line with this observation, although a portion of Eomes$^+$ cells expressed the co-inhibitory receptor TIM-3, the majority of TIM-3$^+$ cells also expressed Ly108 (**Figure 3.7G**), confirming that these cells correspond to activated effector cells rather than exhausted cells.

3.8 Genes associated with Treg cell function are altered when *Icos* is deleted selectively in Treg cells

Since the effects of *Icos* deletion in the CD8$^+$ T cell population seem to be mostly due to a defect in the Treg cell compartment, we decided to analyze the Treg cells in our Foxp3cre transcriptomic dataset. This would give us an idea as to how the Treg cells are altered when they're missing *Icos*. To do this, we isolated and re-clustered all the CD4$^+$ T cells in our Foxp3cre dataset. This resulted in 10 clusters, with no unique clusters associated with either genotype (**Figure 3.8A**). Consistent with our previous T cell data, there were three *Foxp3*$^+$ Treg cell clusters which were either *Cd44*$^-$*Sell*$^+$, *Cd44*$^+$*Sell*$^+$, or *Cd44*$^+$*Sell*$^-$ (**Figure 3.8B**). In addition, since cluster 0 is *Cd44*-, we chose to focus the downstream analysis on clusters 3 and 4, which were *Cd44*$^+$*Sell*$^+$, and *Cd44*$^+$*Sell*$^-$, respectively (**Figure 3.8B**). We next looked at the expression of key Treg cell genes in these populations, and compared their expression between control and knockout samples. Expression of *Il2ra* (CD25), *Tnfrsf18* (GITR), *Ctla4*, *Gzmb*, and *Il10* (IL-10) was elevated in cluster 3 of the knockout sample, whereas, in cluster 4, expression of *Il2ra*, *Tnfrsf18, Pdcd1*, and *Il10* was elevated in the knockout sample (**Figure 3.8C**). On the other hand, the expression of *Ikzf2* (Helios) and *Entpd1* (CD39) were unchanged (**Figure 3.8C**). In addition, *Cd44* was downregulated in the knockout for both clusters, however, this decrease was not observed at the protein level **(Figure 3.5D)**. Furthermore, when comparing between control and knockout samples, *Ccr3* and *Cxcl3* were identified as some of the genes that are significantly upregulated in clusters 3 and 4 in the *Foxp3*^{cre}*Icos*$^{f/f}$ mouse, and *Il18r1*

(IL-18Rα) was found to be downregulated (**Figure 3.8D**). Overall, these data suggest that the expression of many genes important for Treg function, as well as that of cytokines, chemokines, and their receptors, are altered when *Icos* is lost, which could be affecting Treg cell function and, as a result, the $CD8^+$ T cell population.

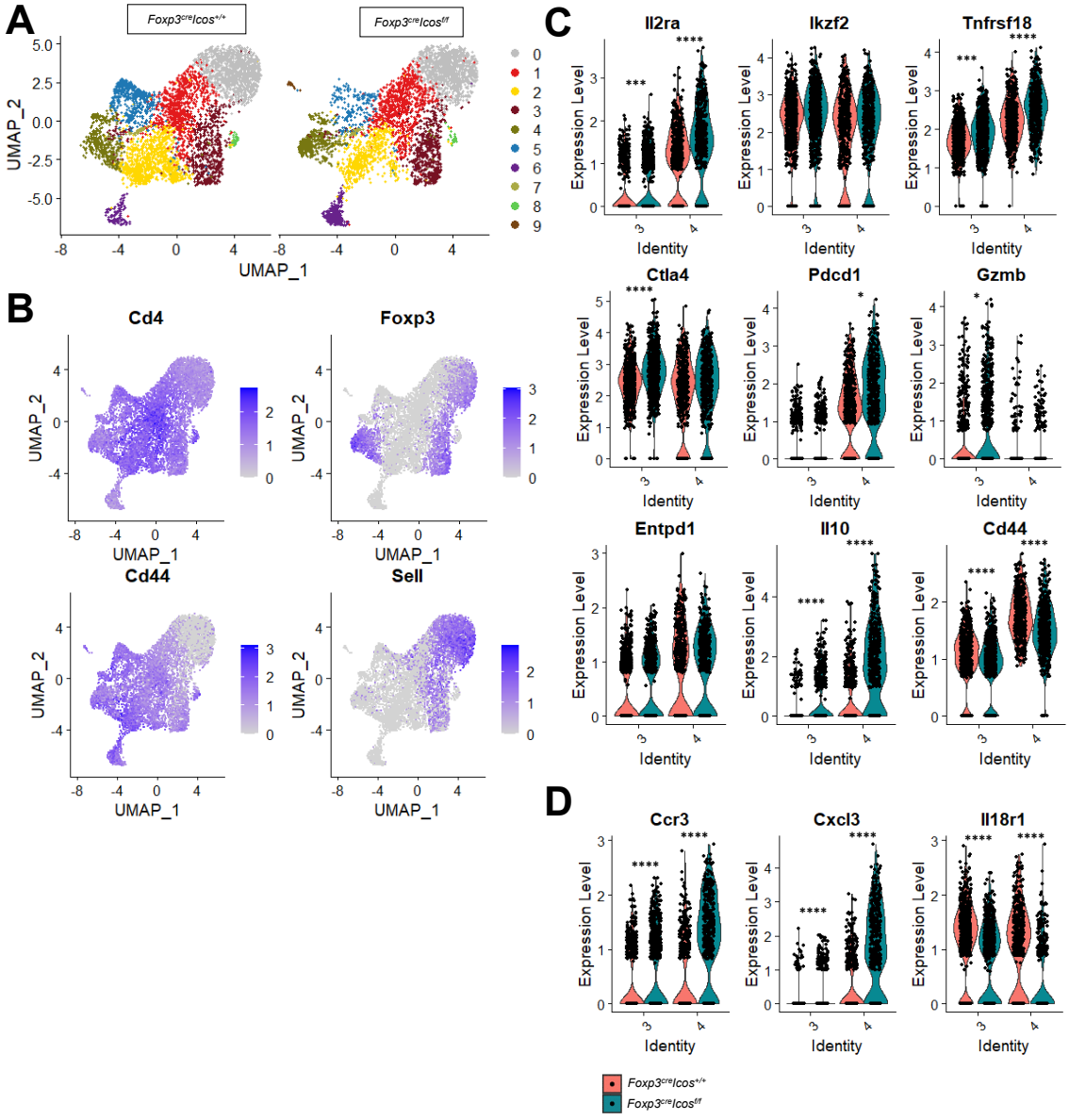

Figure 3.8 Expression of Treg-associated genes is altered when *Icos* is lost in Treg cells. Single-cell RNA sequencing analysis of sorted tumor-infiltrating T cells from one *Foxp3*^{cre}*Icos*$^{+/+}$ and one *Foxp3*^{cre}*Icos*$^{f/f}$ mouse 10 days post-challenge with B16-OVA melanoma cells as in Figure 3.1A. (A) UMAP projections of $CD4^+$ T cell clusters in *Foxp3*^{cre}*Icos*$^{+/+}$ and *Foxp3*^{cre}*Icos*$^{f/f}$ mice. Feature plots of *Cd4, Foxp3, Cd44, Sell* expression. (B) Feature plots of *Cd4*, *Foxp3*, *Cd44, Sell* expression. (C) Violin plots *of Il2ra, Ikzf2, Tnfrsf18, Ctla4, Pdcd1, Gzmb, Entpd1, Il10. Cd44* expression in clusters 3 and 4. (D) Violin plots *of Ccr3, Cxcl3, Il18r1* expression in clusters 3 and 4. Each dot corresponds to one cell. **p*<0.05, ****p*<0.001, *****p*<0.0001.

Chapter 4: Discussion

In this study, we investigated the role of ICOS in T cells in a murine model of metastatic melanoma using regulatory T cell-specific and total T cell-specific conditional deletions of the *Icos* gene. Preliminary data of ours have shown that tumor burden is decreased when *Icos* is deleted in Treg cells, which was not observed in the T cell-specific deletion. This supports the notion that ICOS has a differential role in different T cell subsets in the tumor, as a deletion of *Icos* in all T cells is likely impairing effector T cell populations, such as $CD8^+$ T cells and Th1 cells, in addition to Treg cells.

A deeper look into the dynamics of the T cell populations in tumor-bearing lungs via single-cell transcriptomic analysis revealed two distinct activated effector populations characterized in part by their differential expression of the transcription factors T-bet and Eomes. Notably, *Eomes* mRNA was elevated when *Icos* was deleted in both conditional knockout models, a phenotype we also observed at the protein level in the Foxp3cre model. Eomes is known to be important for CTL development, with studies showing that its expression in $CD8^+$ T cells is essential for the expression of the cytotoxic molecule perforin and the antitumor cytokine IFN-γ[21, 27]. This role for Eomes is consistent with our finding that $Gzmb^+Prf^+$ activated $CD8^+$ T cells are enriched in $Foxp3^{cre}Icos^{-/-}$ mice. However, at the transcriptional level, the expression of perforin and IFN-γ were unchanged in the $Eomes^{hi}$ cluster, even though *Eomes* was significantly upregulated. A possible explanation for this could be the discrepancy between mRNA and protein expression. Differences in mRNA do not always accurately reflect changes in protein product, as multiple levels of post-transcriptional regulation occur between the mRNA and protein stage[100, 101]. Therefore, although transcriptomic data can be informative, changes at the protein level should be confirmed in order to prove that mRNA expression translates into functional differences. Along these lines,

just as granzyme B and perforin protein levels did not coincide with the mRNA expression in our transcriptomic data for cluster 1, it is also possible that IFN-γ behaves similarly. In order to determine if IFN-γ expression by $CD8^+$ T cells is affected by *Icos* deletion, which is expected due to the observed upregulation in Eomes at the protein level, a tumor experiment using the Foxp3cre model should be performed, where the expression of IFN-γ will be assessed by flow cytometry to determine whether IFN-γ is affected when Treg cells are deficient for *Icos.* This would provide further evidence for the protumor role of $ICOS^+$ Treg cells.

In addition, granzyme B mRNA was slightly reduced in the knockout sample of cluster 2 in the Foxp3cre model, although not significantly, which coincides with the downregulation of T-bet mRNA in this population. This is consistent with previous data that show that granzyme B expression is governed by T-bet[27]. Also fitting into this, we found that T-bet was downregulated at the protein level when *Icos* was deleted in the Foxp3cre model. However, there were significantly more $Gzmb^+$ cells in the knockout. There are a few possible explanations for this. For one, this could be explained by the potential differences between mRNA and protein expression. Another possibility is that the $Gzmb^+Prf^+$ population assessed at the protein level included both the $Eomes^{hi}$ and $T\text{-}bet^{hi}$ populations seen in the transcriptomic datasets and this overall increase in granzyme B at the protein level does not reflect the changes occurring in the individual $T\text{-}bet^{hi}$ population. Along these lines, it is possible that the decrease in $T\text{-}bet^+$ cells that was seen in the knockout of both the transcriptomic and flow cytometry data does not majorly affect the overall cytotoxicity of $CD8^+$ T cells due to the expansion of $Eomes^+$ cells. In this case, $Eomes^+$ cells displaying higher cytotoxic function would compensate for the loss of $T\text{-}bet^+$ cells. This is consistent with a key study in which Eomes overexpression *in vitro* was sufficient to induce the expression of granzyme B in the absence of T-bet[21]. Therefore, the increase in $Eomes^+$ cells could be driving the enhanced cytotoxic phenotype of CTLs.

Furthermore, our transcriptomic data in the CD4cre model also revealed an increase in *Eomes* expression in the Eomes^{hi} cluster when *Icos* was lost in all T cells. This was also observed at the protein level and was accompanied by an increase in the percentage of Gzmb^{+}Prf^{+} cells. However, the increase in this population was not significant. This could be due to biological variation among the mice used, which could have resulted in one mouse not experiencing this effect. Another plausible explanation for this difference between the Foxp3cre and CD4cre deletion models could be that a loss of *Icos* in CD8^{+} T cells, as is the case in the CD4cre model, impairs their cytotoxic ability to a certain extent. Our adoptive transfer experiment confirmed this, as there was a significant decrease in the percentage of Gzmb^{+}Prf^{+} ICOS-KO OT1 cells compared to ICOS-Het OT1 cells. Despite this, tumor nodule number was similar between groups, which could be due to other effects of *Icos* deletion in CD8^{+} OT1 T cells, such as impaired IFN-γ expression. IFN-γ expression in OT1 cells was not assessed in our study, but could be an interesting parameter to analyze in a future adoptive transfer experiment. Additionally, other than any additional effector CD8^{+} T cell mechanisms that could be impaired in ICOS-KO OT1 cells, limitations of the adoptive transfer experiment could account for discrepancies between nodule number and percentage of Gzmb^{+}Prf^{+} cells. For one, there were only three mice per experimental group. Due to biological variation between recipient mice, this small sample size may not be representative of the overall effect of *Icos* deletion in OT1 cells. In addition, although 1 x 10^{6} OT1 cells were injected into each mouse, very few CD45.2^{+} donor cells were present in the lungs at the time of analysis, with only a portion of those expressing granzyme B and perforin. Therefore, the frequency of Gzmb^{+}Prf^{+} OT1 cells may not be representative of a true defect in CD8^{+} T cells lacking *Icos*. To acquire more reliable data, the adoptive transfer experiment performed in this study will need to be further optimized and repeated.

Moreover, Eomes expression was not significantly altered between ICOS-Het and ICOS-KO OT1 cells. This suggests that Eomes upregulation observed in the polyclonal $CD8^+$ T cells in the Foxp3cre and CD4cre deletion models is due to a loss of *Icos* in Treg cells. In order to test this, another adoptive transfer experiment can be performed in which OT1 cells sufficient for *Icos* are injected into recipient mice that have Treg cells either sufficient of deficient for *Icos*. In this way, the impact of *Icos* deletion on OT1 cells can be further understood.

Furthermore, there were some differences between the Foxp3cre and CD4cre transcriptomic datasets. Whereas most effector genes studied were decreased in the knockout sample in the T-bet^{hi} cluster in the Foxp3cre model, none of the effector genes were significantly reduced in the corresponding cluster in the CD4cre dataset. In fact, there are some opposing effects, as *Cx3cr1* was upregulated. This is consistent with *T-bet* expression being unchanged in the knockout sample. Furthermore, perforin and IFN-γ was upregulated in the knockout sample for the $Eomes^{hi}$ cluster, which is consistent with the role of Eomes in perforin and IFN-γ induction in $CD8^+$ T cells[21, 27], as *Eomes* is also upregulated in the knockout of this cluster. However, the CD4cre model is complex as all T cells lose *Icos*. Therefore, the changes in mRNA expression observed in the different $CD8^+$ T cell populations could be due to $CD8^+$ T cell-intrinsic or Treg-mediated effects of *Icos* deletion, which makes it difficult to extract clear conclusions from this data. This is also the case with the flow cytometry data in the CD4cre model. Once way in which this is apparent is in the tumor nodule analysis. Whereas tumor burden was decreased in the Foxp3cre model at a late stage of tumor growth, there was no such difference in the CD4cre model. This suggests that other T cell populations could be impaired when all T cells lose *Icos*. Aside from Treg cells, ICOS has been shown to play a role in the function of $CD8^+$ T cells, Th1 cells, Th17 cells, NKT cells, and γδ T cells[35, 102, 103]. Thus, the effects of *Icos* deletion in these populations could explain why tumor nodule number is

unaffected in the CD4cre model, despite the observed increase in the cytotoxic phenotype of the $CD8^+$ T cells. To explore this idea, we could identify and analyze these cells in our single-cell RNA sequencing datasets, as well profile these populations via flow cytometry. This would aid in identifying the reason behind the discrepancy in tumor nodule number between our knockout models, as well as provide further evidence that the increase in CTL cytotoxicity is a major factor impacting tumor burden.

Another interesting finding in our transcriptomic data is that the $Eomes^{hi}$ cluster most likely corresponds to activated effector cells as opposed to exhausted cells, despite the expression of inhibitory receptors. When comparing the two effector clusters in both transcriptomic datasets, the $Eomes^{hi}$ population expressed the highest level of the co-inhibitory receptors PD-1, LAG3, and CTLA4. In the tumor microenvironment, these proteins are most often associated with exhausted and dysfunctional $CD8^+$ T cells that have dampened effector functions, with these terminally dysfunctional T cells described in the literature as being $Ly108^-$ [104]. Additionally, Eomes has been found to play a role in the T cell exhaustion process, with multiple studies linking Eomes expression to T cell dysfunction at late stages of T cell differentiation[32, 105]. However, our transcriptomic data revealed that the $Eomes^{hi}$ population does express Ly108 in addition to the inhibitory receptors. This was also confirmed at the protein level, as most $Eomes^+$ $CD8^+$ T cells also expressed Ly108. Importantly, co-inhibitory receptors are involved in immune homeostasis, as they are expressed following TCR stimulation and function to dampen T cell activation and prevent excessive T cell responses[106]. Consistent with this, co-inhibitory receptors PD-1 and CTLA4 were found to be expressed on T cells following activation[107, 108]. In addition, there is evidence that inhibitory receptor expression is an indicator of T cell differentiation and function as opposed to exhaustion[109]. Therefore, the coexpression of inhibitory receptors, effector genes, and Ly108 in the $Eomes^{hi}$ population, in addition to the fact that these lymphocytes were taken from lungs at an early

stage of tumor growth, indicates that these cells are activated rather than exhausted. This suggests that the increase in Eomes expression is an indication of enhanced T cell maturation, as opposed to enhanced exhaustion.

Overall, our analysis of $CD8^+$ T cells in the tumor microenvironment suggests that the loss of *Icos* in Treg cells promotes Eomes upregulation and CTL cytotoxicity. However, it is unclear what the role of $ICOS^+$ Treg cells is in this process. Our Foxp3cre transcriptomic data revealed that the cluster proportions of the two effector $CD8^+$ T cell populations are different between genotypes, with the T-bet^{hi} population being decreased and the $Eomes^{hi}$ population being increased when *Icos* is lost in Tregs. One possibility is that these two clusters represent different stages of $CD8^+$ T cell differentiation in the tumor microenvironment, with one population giving rise to the other. In our model, the cells of the T-bet^{hi} cluster could be differentiating into the cells of the $Eomes^{hi}$ cluster. This is supported by evidence that T-bet is expressed at earlier stages of $CD8^+$ T cell differentiation *in vitro*, and that this is later followed by Eomes upregulation[27]. Our data suggest that this could also be occurring *in vivo*. Additionally, it is well-known that Eomes expression increases along the effector to memory cell transition[110, 111, 112], which supports the idea that the T-bet^{hi} population is a precursor for the $Eomes^{hi}$ population. This is also supported by our transcriptomic data in which effector genes are expressed at a lower level in the $Eomes^{hi}$ cluster compared to that of the T-bet^{hi} cluster. Therefore, it appears that the $ICOS^+$ Treg cells could be restraining the differentiation and maturation of CTLs, which results in less Eomes expression and impaired cytotoxicity. This is consistent with a study in which Treg cells were found to inhibit $CD8^+$ T cell maturation by inhibiting the $CD4^+$ T helper cell response[113]. $ICOS^+$ Treg cells could be the regulatory T cells responsible for this. In addition, to determine the relationship between the T-bet^{hi} and $Eomes^{hi}$ clusters, scVelo analysis could be performed on our single-cell transcriptomic data. This is a method of studying cell differentiation in which RNA splicing patterns within cells of

a transcriptomic dataset can be analyzed in order to determine the developmental relationship between cells[114, 115, 116]. This technique would provide insight into the dynamics of the Eomes^{hi} and T-bet^{hi} clusters and, thus, help elucidate the role of ICOS^{+} Treg cells in CD8^{+} T cell differentiation and function.

Furthermore, we also analyzed Treg cell gene expression in our transcriptomic dataset for the Foxp3cre model in order to attempt to explain how Treg cells are altered, and how they could possibly be impacting the dynamics of effector CD8^{+} T cells in a way that ultimately results in decreased tumor burden. Interestingly, there was an increase in most genes known to be important for Treg cell function in the *Foxp3^{cre}Icos$^{-/-}$* mouse. Of note, CD25, IL-10, and GITR were upregulated in the effector Treg cell cluster of the knockout sample, and other genes such as Helios and CD39 were unchanged. This suggests that Treg cells may not be functionally impaired when ICOS is missing in the tumor-infiltrating Treg cells. This is consistent with evidence showing that a deletion of *Icos* in Treg cells at steady state does not severely impact the expression of key Treg cell genes[81]. This could also be occurring in our tumor model. Interestingly, this study also found that CD25 was elevated in ICOS-deficient Treg cells, a phenotype we also observed in our transcriptomic data. As CD25 is important for the suppressive function of Treg cells[117], this suggests that their suppressive function could be enhanced when *Icos* is deleted. Therefore, the Treg cells in the TME don't seem to be functionally impaired. However, an important limitation of our transcriptomic data is the sample size. Due to only having one mouse per genotype, it is possible that the changes occurring between the control and knockout samples are not representative of the entire population. Therefore, our transcriptomic results need to be confirmed by analyzing the expression of Treg cell markers at the protein level via flow cytometry.

In addition, we found that the frequency of Treg cells in the lung was significantly decreased in the knockout of the Foxp3cre model. Together with our transcriptomic data where Treg cell function appears to unaffected or even enhanced in the knockout sample, this suggests that the major effect of ICOS deficiency in Treg cells is an issue with tumor-infiltration or potentially with Treg cell survival within the tumor. Importantly, this difference was not seen in the single-cell dataset due to the methodology used. Treg cells were added in equal proportions to the effector T cells in order to best analyze differences in gene expression between genotypes, and this abrogated the difference in Treg cell infiltration observed by flow cytometry.

Interestingly, we found that Treg cells in our Foxp3cre transcriptomic dataset express the chemokine receptor Ccr3 and the cytokine Cxcl3, and that the expression of these genes was increased when Tregs lost *Icos*. $Ccr3^{+}$ Tregs in cancer have not been characterized, however, Ccr3 has been shown to be expressed in splenic, adipose tissue, and colonic Treg cells[118, 119]. In cancer, Ccr3 has been associated with the recruitment of immune cells to the tumor[120]. Therefore, the increase in Ccr3 expression in Tregs following *Icos* deletion could be modulating the immune response in the tumor. Additionally, Cxcl3 has not been studied in Treg cells, but its receptor, CXCR2, has been shown to be expressed in melanoma cells, and it has a known role in immune cell recruitment, angiogenesis, and metastasis[121]. Therefore, it is possible that Cxcl3 expression by Tregs is involved in these processes. Furthermore, we found that IL-18R1 was downregulated in the Treg cells of the $Foxp3^{cre}Icos^{-/-}$ mouse. IL-18R1 signalling has been shown to be important for the capacity of Tregs to suppress colitis[122]. Additionally, dendritic cell-derived IL-18 was found to promote Treg cell differentiation in mice infected with *Helicobacter pylori*, and Treg cells from $Il18^{-/-}$ and $Il18r1^{-/-}$ mice were unable to control airway inflammation in mice[123]. This suggests that a deficiency in IL-18 signalling can impair Treg cell function, which could also be occurring when Treg cells lose

Icos in our tumor model. Therefore, *Icos* deletion in Treg cells appears to impact their expression of chemokines and their receptors, as well as cytokines, and this could be impacting their localization, infiltration, and function in the TME.

Finally, an important caveat in this study is the use of OVA as a tumor antigen. We used this highly immunogenic surrogate antigen to provoke strong T cell responses to reveal any potential impacts of ICOS deficiency. This also allowed us to monitor the behaviour transgenic OT-I cells after adoptive transfer. However, this may not accurately represent the actual response to tumor antigens in naturally arising cancers. Therefore, the dual role of ICOS observed using our B16-OVA model may be less pronounced in other tumor models. Further studies could be done using less immunogenic tumor models in order to address this possible discrepancy.

Overall, our results suggest that a loss of ICOS in Treg cells could be impacting their function by impairing their infiltration in the TME. This in turn promotes the expansion of $Eomes^+$ $CD8^+$ T cells and enhances their cytotoxicity, which ultimately results in decreased tumor burden at a late stage of tumor growth. Finally, whereas a deletion of *Icos* in total T cells recapitulated some of these phenotypes, tumor burden remained unchanged, probably due to the impaired function of other ICOS-expressing antitumor T cell subsets.

Chapter 5: Conclusion

The objectives of this study were to determine the role of ICOS in antitumor T cell immunity by elucidating the differential requirements for ICOS in different T cell subsets. To do this, we used pan-T cell-specific and Treg cell-specific models of *Icos* deletion in a model of murine metastatic melanoma. Preliminary results showed that a Treg cell-specific deletion of *Icos* resulted in decreased tumor burden in mice, whereas a pan-T cell-specific deletion did not. Using single-cell transcriptomic analysis, we identified two populations of effector CTLs in the TME, and found that loss of ICOS in Treg cells promoted the expansion of the $Eomes^{hi}$ population. This was confirmed at the protein level and was associated with increased CTL cytotoxicity. Additionally, even though a loss of *Icos* in all T cells recapitulated some of the phenotypes seen in the Foxp3cre model, we found ICOS to be important for CTL cytotoxicity in a $CD8^+$ T cell-intrinsic manner. Despite this, the impairment of Treg cells following *Icos* deletion seems to be the main driver of Eomes upregulation and increased cytotoxicity in our tumor model. Therefore, our data suggest that ICOS plays a primarily protumor role in the TME by inhibiting effector T cell responses. However, the mechanism behind the regulation of these responses by $ICOS^+$ Treg cells remains unclear and needs to be studied further. Our findings could help inform the use of anti-ICOS antibodies in clinical trials, as ICOS agonists are likely promoting the protumor effects of Treg cells and limiting the antitumor functions of effector cells.

Supplementary Figures

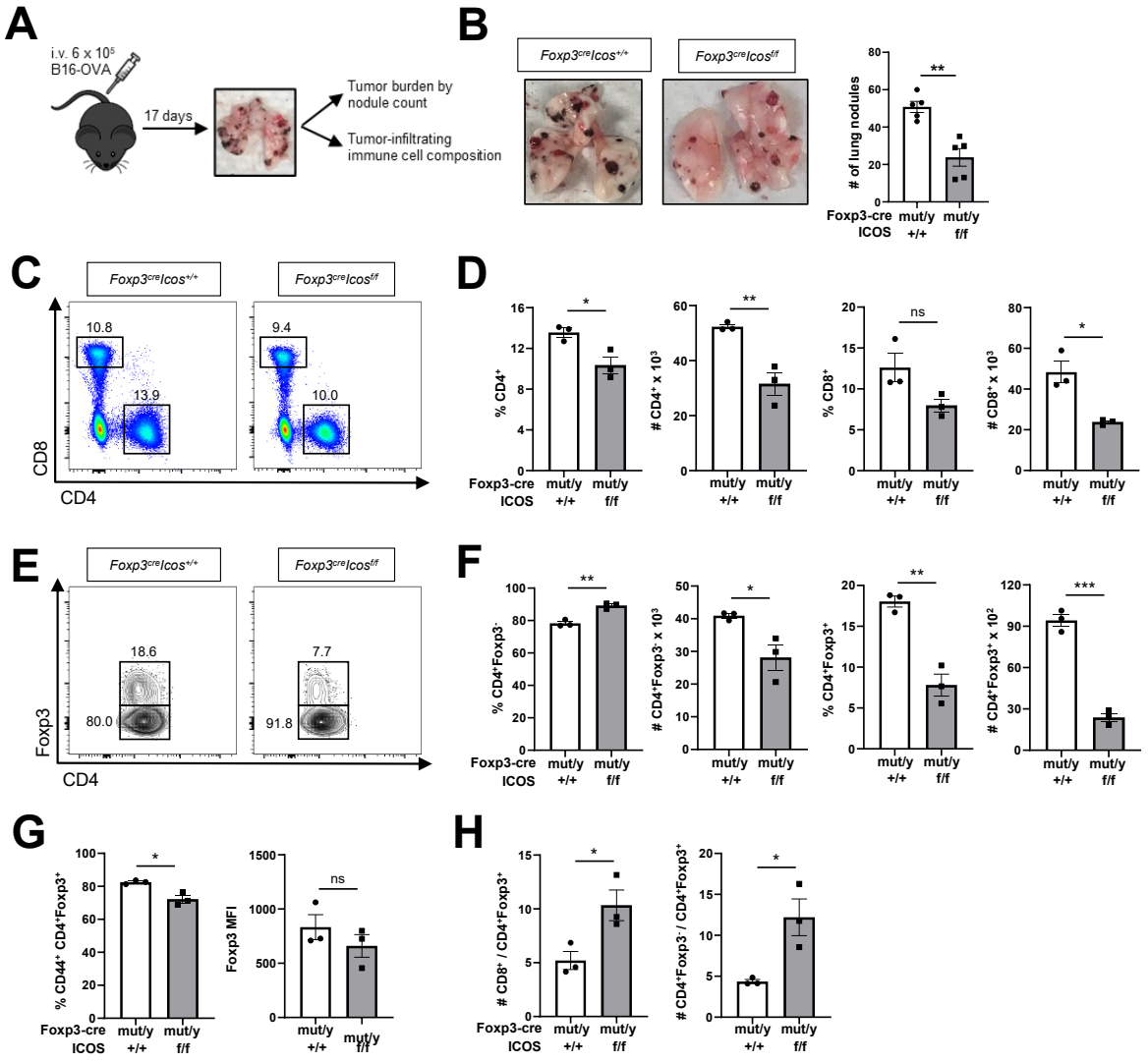

Supplemental Figure 3.1 Reduced tumor burden and augmented Teff:Treg ratio in Treg-specific ICOS deficient mice. (A) Experimental setup for murine model of metastatic melanoma. 8- to 11-weeks old *Foxp3*$^{YFP\text{-}cre}$*Icos*$^{+/+}$ (abbreviated as *Foxp3*^{cre}*Icos*$^{+/+}$) and *Foxp3*$^{YFP\text{-}cre}$*Icos*$^{f/f}$ (abbreviated as *Foxp3*^{cre}*Icos*$^{f/f}$) male mice were challenged with tumor cells as in (A) (n = 5 each). (B) Representative images of lung tumor burden in *Foxp3*^{cre}*Icos*$^{+/+}$ vs. *Foxp3*^{cre}*Icos*$^{f/f}$ mice, and statistical analysis of lung nodule count. (C-H) Flow cytometry analysis of tumor-infiltrating immune cells as obtained from mouse lungs in (B). (C) Representative flow cytometry plots of CD4$^+$ and CD8$^+$ cells pre-gated on CD45$^+$ cells. (D) Statistical analysis of CD4$^+$ and CD8$^+$ cell percentage and numbers. (E) Representative flow cytometry plots of non-Treg (CD4$^+$Foxp3$^-$) and Treg (CD4$^+$Foxp3$^+$) cells pre-gated on CD4$^+$ cells. (F) non-Treg CD4$^+$ and Treg cells percentage and numbers. (G) Percentage of activated Treg (CD44$^+$CD4$^+$Foxp3$^+$) cells pre-gated on CD4$^+$ cells and Foxp3 mean fluorescence intensity (MFI) in Treg cells. (H) Ratio of CD8$^+$ effector T cells to Treg cells and non-Treg CD4$^+$ cells to Treg cells. Data shown as mean with error bars denoting SEM, *p<0.05, **p<0.01, ***p<0.001. Data is representative of at least two independent experiments.

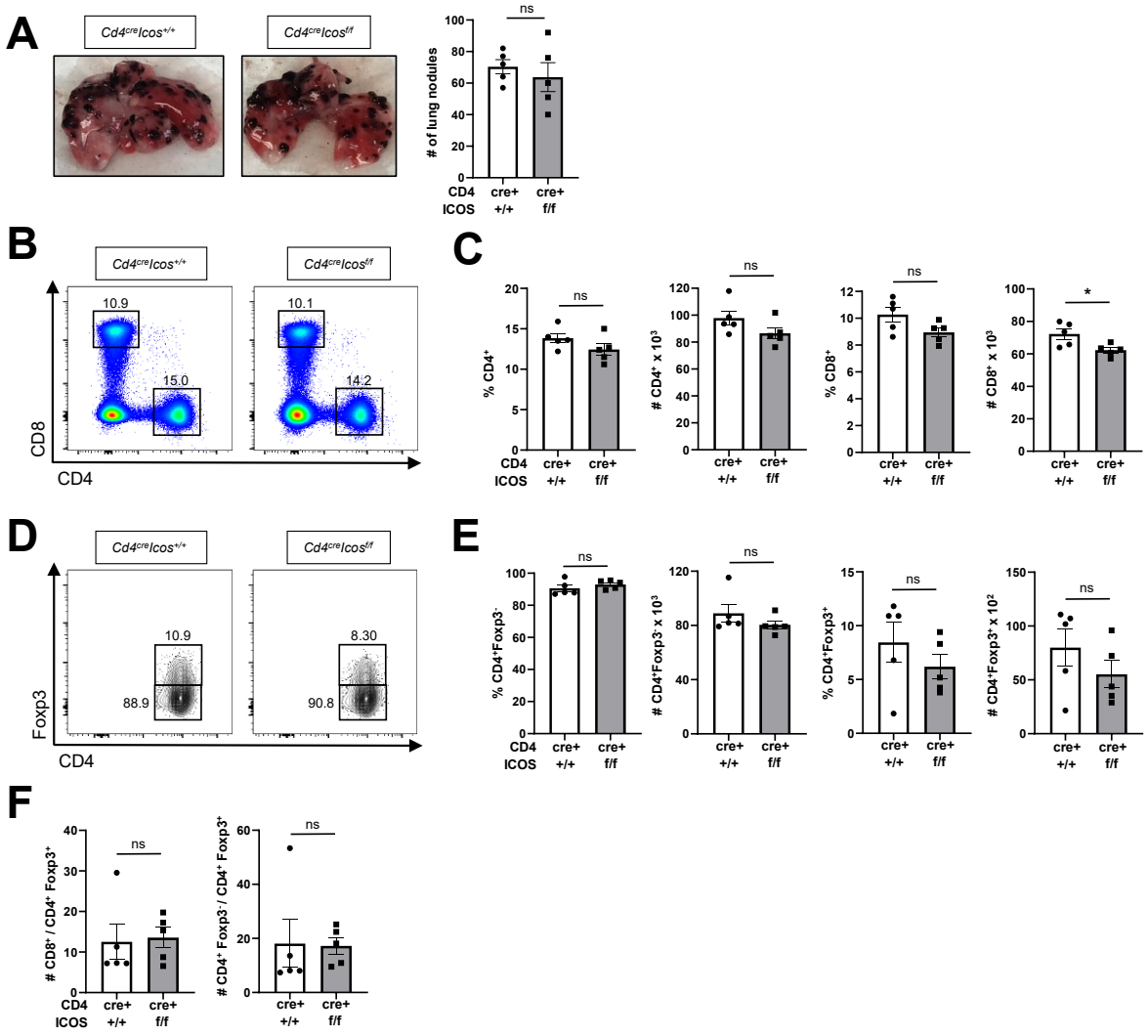

Supplemental Figure 3.2 No significant differences in tumour burden and tumor-infiltrating T cell populations in T cell-specific ICOS deficient mice. 9- to 12-weeks old female *Cd4*^{cre}*Icos*$^{+/+}$ and *Cd4*^{cre}*Icos*$^{f/f}$ mice (n = 5 each) that have been co-housed for at least 2 weeks were challenged with tumor cells as in Supplemental Figure 3.2A. (A) Representative images of lung tumor burden in *Cd4*^{cre}*Icos*$^{+/+}$ versus *Cd4*^{cre}*Icos*$^{f/f}$ mice, and statistical analysis of lung nodule count. (B-F) Flow cytometry analysis of tumor-infiltrating immune cells as obtained from mouse lungs in (A). (B) Representative flow cytometry plots of CD4$^+$ and CD8$^+$ cells pre-gated on CD45$^+$ cells. (C) Statistical analysis of CD4$^+$ and CD8$^+$ cell percentage and numbers. (D) Representative flow cytometry plots of non-Treg (CD4$^+$Foxp3$^-$) and Treg (CD4$^+$Foxp3$^+$) cells pre-gated on CD4$^+$ cells. (E) non-Treg CD4$^+$ and Treg cells percentage and numbers. (F) Ratio of CD8$^+$ effector T cells to Treg cells and non-Treg CD4$^+$ cells to Treg cells. Data shown as mean with error bars denoting SEM, ns = not statistically significant. *p<0.05. Data is representative of three independent experiments.

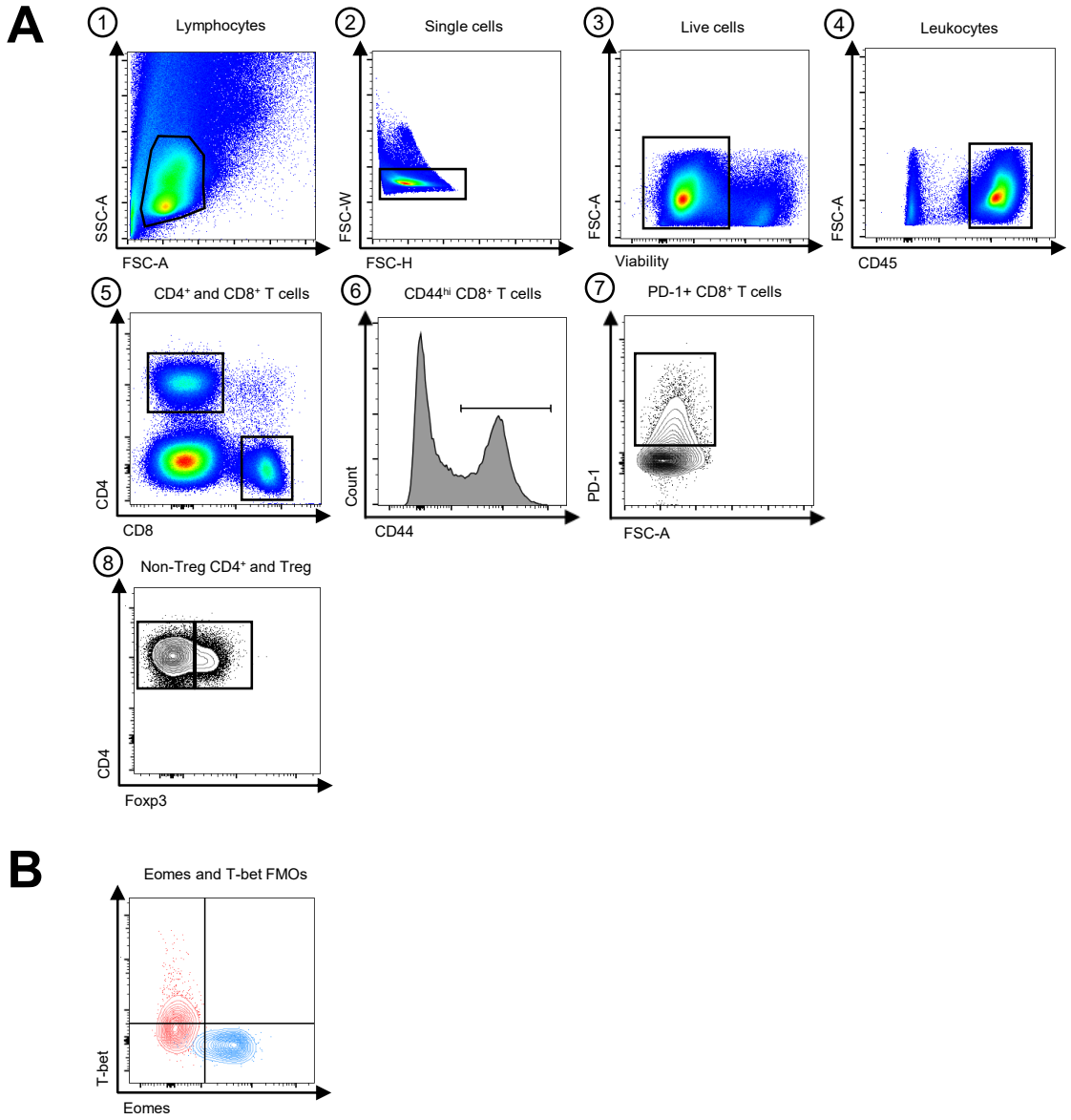

Supplemental Figure 3.3 Gating strategy to identify tumor-infiltrating T cell populations in the lung. (A) Lymphocytes were first gated from total lung cells, followed by the selection of singlets and live cells. $CD45^+$ leukocytes were then gated, followed by tumor-infiltrating $CD4^+$ and $CD8^+$ T cells. To identify tumor-specific $CD8^+$ T cells, $CD44^{hi}$ and PD-1^+ cells were further gated. Finally Tregs and non-Treg $CD4^+$ T cells were gated within the total $CD4^+$ T cells based on Foxp3 expression. (B) Positive Eomes and T-bet signals were determined based on Eomes (red) and T-bet (blue) fluorescence minus one (FMO) controls.

References

1. Ward, J.P., Gubin, M.M. & Schreiber, R.D. The Role of Neoantigens in Naturally Occurring and Therapeutically Induced Immune Responses to Cancer. *Adv Immunol* **130**, 25-74 (2016).

2. Schreiber, R.D., Old, L.J. & Smyth, M.J. Cancer immunoediting: integrating immunity's roles in cancer suppression and promotion. *Science* **331**, 1565-1570 (2011).

3. Beatty, G.L. & Gladney, W.L. Immune escape mechanisms as a guide for cancer immunotherapy. *Clin Cancer Res* **21**, 687-692 (2015).

4. Liu, G., Rui, W., Zhao, X. & Lin, X. Enhancing CAR-T cell efficacy in solid tumors by targeting the tumor microenvironment. *Cell Mol Immunol* **18**, 1085-1095 (2021).

5. Hegde, P.S. & Chen, D.S. Top 10 Challenges in Cancer Immunotherapy. *Immunity* **52**, 17-35 (2020).

6. O'Donnell, J.S., Teng, M.W.L. & Smyth, M.J. Cancer immunoediting and resistance to T cell-based immunotherapy. *Nat Rev Clin Oncol* **16**, 151-167 (2019).

7. Germain, R.N. T-cell development and the CD4-CD8 lineage decision. *Nat Rev Immunol* **2**, 309-322 (2002).

8. Merad, M., Sathe, P., Helft, J., Miller, J. & Mortha, A. The dendritic cell lineage: ontogeny and function of dendritic cells and their subsets in the steady state and the inflamed setting. *Annu Rev Immunol* **31**, 563-604 (2013).

9. Fu, C. & Jiang, A. Dendritic Cells and CD8 T Cell Immunity in Tumor Microenvironment. *Front Immunol* **9**, 3059 (2018).

10. Roberts, E.W. *et al.* Critical Role for CD103(+)/CD141(+) Dendritic Cells Bearing CCR7 for Tumor Antigen Trafficking and Priming of T Cell Immunity in Melanoma. *Cancer Cell* **30**, 324-336 (2016).

11. Voskoboinik, I., Whisstock, J.C. & Trapani, J.A. Perforin and granzymes: function, dysfunction and human pathology. *Nature Reviews Immunology* **15**, 388-400 (2015).

12. Zhou, Z. *et al.* Granzyme A from cytotoxic lymphocytes cleaves GSDMB to trigger pyroptosis in target cells. *Science* **368**, eaaz7548 (2020).

13. Lopez, J.A. *et al.* Perforin forms transient pores on the target cell plasma membrane to facilitate rapid access of granzymes during killer cell attack. *Blood* **121**, 2659-2668 (2013).

14. Kägi, D. *et al.* Cytotoxicity mediated by T cells and natural killer cells is greatly impaired in perforin-deficient mice. *Nature* **369**, 31-37 (1994).

15. Kägi, D. *et al.* Fas and perforin pathways as major mechanisms of T cell-mediated cytotoxicity. *Science* **265**, 528-530 (1994).

16. Lowin, B., Hahne, M., Mattmann, C. & Tschopp, J. Cytolytic T-cell cytotoxicity is mediated through perforin and Fas lytic pathways. *Nature* **370**, 650-652 (1994).

17. Jorgovanovic, D., Song, M., Wang, L. & Zhang, Y. Roles of IFN-γ in tumor progression and regression: a review. *Biomarker Research* **8**, 49 (2020).

18. Bhat, P., Leggatt, G., Waterhouse, N. & Frazer, I.H. Interferon-γ derived from cytotoxic lymphocytes directly enhances their motility and cytotoxicity. *Cell Death & Disease* **8**, e2836-e2836 (2017).

19. Qin, Z. *et al.* A critical requirement of interferon gamma-mediated angiostasis for tumor rejection by CD8+ T cells. *Cancer Res* **63**, 4095-4100 (2003).

20. Kaech, S.M. & Cui, W. Transcriptional control of effector and memory CD8+ T cell differentiation. *Nat Rev Immunol* **12**, 749-761 (2012).

21. Pearce, E.L. *et al.* Control of effector CD8+ T cell function by the transcription factor Eomesodermin. *Science* **302**, 1041-1043 (2003).

22. Szabo, S.J. *et al.* A novel transcription factor, T-bet, directs Th1 lineage commitment. *Cell* **100**, 655-669 (2000).

23. Sullivan, B.M., Juedes, A., Szabo, S.J., von Herrath, M. & Glimcher, L.H. Antigen-driven effector CD8 T cell function regulated by T-bet. *Proc Natl Acad Sci U S A* **100**, 15818-15823 (2003).

24. Joshi, N.S. *et al.* Inflammation directs memory precursor and short-lived effector CD8(+) T cell fates via the graded expression of T-bet transcription factor. *Immunity* **27**, 281-295 (2007).

25. Ryan, K., Garrett, N., Mitchell, A. & Gurdon, J.B. Eomesodermin, a key early gene in Xenopus mesoderm differentiation. *Cell* **87**, 989-1000 (1996).

26. Russ, A.P. *et al.* Eomesodermin is required for mouse trophoblast development and mesoderm formation. *Nature* **404**, 95-99 (2000).

27. Cruz-Guilloty, F. *et al.* Runx3 and T-box proteins cooperate to establish the transcriptional program of effector CTLs. *J Exp Med* **206**, 51-59 (2009).

28. Prier, J.E. *et al.* Early T-BET Expression Ensures an Appropriate CD8⁺ Lineage–Specific Transcriptional Landscape after Influenza A Virus Infection. *The Journal of Immunology* **203**, 1044-1054 (2019).

29. Intlekofer, A.M. *et al.* Anomalous type 17 response to viral infection by CD8+ T cells lacking T-bet and eomesodermin. *Science* **321**, 408-411 (2008).

30. Wherry, E.J. T cell exhaustion. *Nature Immunology* **12**, 492-499 (2011).

31. Wherry, E.J. & Kurachi, M. Molecular and cellular insights into T cell exhaustion. *Nature Reviews Immunology* **15**, 486-499 (2015).

32. Paley, M.A. *et al.* Progenitor and terminal subsets of CD8+ T cells cooperate to contain chronic viral infection. *Science* **338**, 1220-1225 (2012).

33. Wei, S.C., Duffy, C.R. & Allison, J.P. Fundamental Mechanisms of Immune Checkpoint Blockade Therapy. *Cancer Discov* **8**, 1069-1086 (2018).

34. Marin-Acevedo, J.A., Kimbrough, E.O. & Lou, Y. Next generation of immune checkpoint inhibitors and beyond. *Journal of Hematology & Oncology* **14**, 45 (2021).

35. Kim, H.J. & Cantor, H. CD4 T-cell subsets and tumor immunity: the helpful and the not-so-helpful. *Cancer Immunol Res* **2**, 91-98 (2014).

36. Smith, C.M. *et al.* Cognate CD4+ T cell licensing of dendritic cells in CD8+ T cell immunity. *Nature Immunology* **5**, 1143-1148 (2004).

37. Ridge, J.P., Di Rosa, F. & Matzinger, P. A conditioned dendritic cell can be a temporal bridge between a CD4+ T-helper and a T-killer cell. *Nature* **393**, 474-478 (1998).

38. Tay, R.E., Richardson, E.K. & Toh, H.C. Revisiting the role of CD4+ T cells in cancer immunotherapy—new insights into old paradigms. *Cancer Gene Therapy* **28**, 5-17 (2021).

39. Ahrends, T. *et al.* CD4(+) T Cell Help Confers a Cytotoxic T Cell Effector Program Including Coinhibitory Receptor Downregulation and Increased Tissue Invasiveness. *Immunity* **47**, 848-861.e845 (2017).

40. Wang, J.C. & Livingstone, A.M. Cutting edge: CD4+ T cell help can be essential for primary CD8+ T cell responses in vivo. *J Immunol* **171**, 6339-6343 (2003).

41. Braumüller, H. *et al.* T-helper-1-cell cytokines drive cancer into senescence. *Nature* **494**, 361-365 (2013).

42. Bennett, C.L. *et al.* The immune dysregulation, polyendocrinopathy, enteropathy, X-linked syndrome (IPEX) is caused by mutations of FOXP3. *Nat Genet* **27**, 20-21 (2001).

43. Brunkow, M.E. *et al.* Disruption of a new forkhead/winged-helix protein, scurfin, results in the fatal lymphoproliferative disorder of the scurfy mouse. *Nat Genet* **27**, 68-73 (2001).

44. Josefowicz, S.Z., Lu, L.F. & Rudensky, A.Y. Regulatory T cells: mechanisms of differentiation and function. *Annu Rev Immunol* **30**, 531-564 (2012).

45. Chen, W. *et al.* Conversion of peripheral CD4+CD25- naive T cells to CD4+CD25+ regulatory T cells by TGF-beta induction of transcription factor Foxp3. *J Exp Med* **198**, 1875-1886 (2003).

46. Ohue, Y. & Nishikawa, H. Regulatory T (Treg) cells in cancer: Can Treg cells be a new therapeutic target? *Cancer Sci* **110**, 2080-2089 (2019).

47. Seed, R.I. *et al.* A tumor-specific mechanism of T(reg) enrichment mediated by the integrin αvβ8. *Sci Immunol* **6** (2021).

48. Fridman, W.H., Pagès, F., Sautès-Fridman, C. & Galon, J. The immune contexture in human tumours: impact on clinical outcome. *Nature Reviews Cancer* **12**, 298-306 (2012).

49. Walker, L.S. & Sansom, D.M. The emerging role of CTLA4 as a cell-extrinsic regulator of T cell responses. *Nat Rev Immunol* **11**, 852-863 (2011).

50. Qureshi, O.S. *et al.* Trans-endocytosis of CD80 and CD86: a molecular basis for the cell-extrinsic function of CTLA-4. *Science* **332**, 600-603 (2011).

51. Cao, X. *et al.* Granzyme B and perforin are important for regulatory T cell-mediated suppression of tumor clearance. *Immunity* **27**, 635-646 (2007).

52. Deaglio, S. *et al.* Adenosine generation catalyzed by CD39 and CD73 expressed on regulatory T cells mediates immune suppression. *J Exp Med* **204**, 1257-1265 (2007).

53. Hutloff, A. *et al.* ICOS is an inducible T-cell co-stimulator structurally and functionally related to CD28. *Nature* **397**, 263-266 (1999).

54. Panneton, V., Chang, J., Witalis, M., Li, J. & Suh, W.K. Inducible T-cell co-stimulator: Signaling mechanisms in T follicular helper cells and beyond. *Immunol Rev* **291**, 91-103 (2019).

55. Lownik, J.C. *et al.* ADAM10-Mediated ICOS Ligand Shedding on B Cells Is Necessary for Proper T Cell ICOS Regulation and T Follicular Helper Responses. *J Immunol* **199**, 2305-2315 (2017).

56. Smigiel, K.S. *et al.* CCR7 provides localized access to IL-2 and defines homeostatically distinct regulatory T cell subsets. *Journal of Experimental Medicine* **211**, 121-136 (2013).

57. Maazi, H. *et al.* ICOS:ICOS-ligand interaction is required for type 2 innate lymphoid cell function, homeostasis, and induction of airway hyperreactivity. *Immunity* **42**, 538-551 (2015).

58. Qian, X. *et al.* The ICOS-ligand B7-H2, expressed on human type II alveolar epithelial cells, plays a role in the pulmonary host defense system. *Eur J Immunol* **36**, 906-918 (2006).

59. Wiendl, H. *et al.* Muscle fibres and cultured muscle cells express the B7.1/2-related inducible co-stimulatory molecule, ICOSL: implications for the pathogenesis of inflammatory myopathies. *Brain* **126**, 1026-1035 (2003).

60. Gigoux, M. *et al.* Inducible costimulator promotes helper T-cell differentiation through phosphoinositide 3-kinase. *Proc Natl Acad Sci U S A* **106**, 20371-20376 (2009).

61. Leconte, J., Bagherzadeh Yazdchi, S., Panneton, V. & Suh, W.K. Inducible costimulator (ICOS) potentiates TCR-induced calcium flux by augmenting PLCγ1 activation and actin remodeling. *Mol Immunol* **79**, 38-46 (2016).

62. Pedros, C. *et al.* A TRAF-like motif of the inducible costimulator ICOS controls development of germinal center TFH cells via the kinase TBK1. *Nat Immunol* **17**, 825-833 (2016).

63. Stone, E.L. *et al.* ICOS coreceptor signaling inactivates the transcription factor FOXO1 to promote Tfh cell differentiation. *Immunity* **42**, 239-251 (2015).

64. Wallin, J.J., Liang, L., Bakardjiev, A. & Sha, W.C. Enhancement of CD8+ T cell responses by ICOS/B7h costimulation. *J Immunol* **167**, 132-139 (2001).

65. Liu, X. *et al.* B7H costimulates clonal expansion of, and cognate destruction of tumor cells by, CD8(+) T lymphocytes in vivo. *J Exp Med* **194**, 1339-1348 (2001).

66. Vidric, M., Bladt, A.T., Dianzani, U. & Watts, T.H. Role for inducible costimulator in control of Salmonella enterica serovar Typhimurium infection in mice. *Infect Immun* **74**, 1050-1061 (2006).

67. Peng, C. *et al.* Engagement of the costimulatory molecule ICOS in tissues promotes establishment of CD8(+) tissue-resident memory T cells. *Immunity* **55**, 98-114.e115 (2022).

68. Corgnac, S., Boutet, M., Kfoury, M., Naltet, C. & Mami-Chouaib, F. The Emerging Role of CD8(+) Tissue Resident Memory T (T(RM)) Cells in Antitumor Immunity: A Unique Functional Contribution of the CD103 Integrin. *Front Immunol* **9**, 1904 (2018).

69. Wikenheiser, D.J. & Stumhofer, J.S. ICOS Co-Stimulation: Friend or Foe? *Front Immunol* **7**, 304 (2016).

70. Nouailles, G. *et al.* Impact of inducible co-stimulatory molecule (ICOS) on T-cell responses and protection against Mycobacterium tuberculosis infection. *Eur J Immunol* **41**, 981-991 (2011).

71. Kadkhoda, K. *et al.* Th1 cytokine responses fail to effectively control Chlamydia lung infection in ICOS ligand knockout mice. *J Immunol* **184**, 3780-3788 (2010).

72. Rutitzky, L.I., Ozkaynak, E., Rottman, J.B. & Stadecker, M.J. Disruption of the ICOS-B7RP-1 costimulatory pathway leads to enhanced hepatic immunopathology and increased gamma interferon production by CD4 T cells in murine schistosomiasis. *Infect Immun* **71**, 4040-4044 (2003).

73. Mittrücker, H.W. *et al.* Inducible costimulator protein controls the protective T cell response against Listeria monocytogenes. *J Immunol* **169**, 5813-5817 (2002).

74. Li, D.Y. & Xiong, X.Z. ICOS(+) Tregs: A Functional Subset of Tregs in Immune Diseases. *Front Immunol* **11**, 2104 (2020).

75. Burmeister, Y. *et al.* ICOS controls the pool size of effector-memory and regulatory T cells. *J Immunol* **180**, 774-782 (2008).

76. Landuyt, A.E., Klocke, B.J., Colvin, T.B., Schoeb, T.R. & Maynard, C.L. Cutting Edge: ICOS-Deficient Regulatory T Cells Display Normal Induction of Il10 but Readily Downregulate Expression of Foxp3. *J Immunol* **202**, 1039-1044 (2019).

77. Chen, Y., Shen, S., Gorentla, B.K., Gao, J. & Zhong, X.P. Murine regulatory T cells contain hyperproliferative and death-prone subsets with differential ICOS expression. *J Immunol* **188**, 1698-1707 (2012).

78. Kornete, M., Sgouroudis, E. & Piccirillo, C.A. ICOS-dependent homeostasis and function of Foxp3+ regulatory T cells in islets of nonobese diabetic mice. *J Immunol* **188**, 1064-1074 (2012).

79. Löhning, M. *et al.* Expression of ICOS in vivo defines CD4+ effector T cells with high inflammatory potential and a strong bias for secretion of interleukin 10. *J Exp Med* **197**, 181-193 (2003).

80. Kohyama, M. *et al.* Inducible costimulator-dependent IL-10 production by regulatory T cells specific for self-antigen. *Proc Natl Acad Sci U S A* **101**, 4192-4197 (2004).

81. Chang, J. *et al.* ICOS-Deficient Regulatory T Cells Can Prevent Spontaneous Autoimmunity but Are Impaired in Controlling Acute Inflammation. *J Immunol* **209**, 301-309 (2022).

82. Liakou, C.I. *et al.* CTLA-4 blockade increases IFNgamma-producing CD4+ICOShi cells to shift the ratio of effector to regulatory T cells in cancer patients. *Proc Natl Acad Sci U S A* **105**, 14987-14992 (2008).

83. Vonderheide, R.H. *et al.* Tremelimumab in combination with exemestane in patients with advanced breast cancer and treatment-associated modulation of inducible costimulator expression on patient T cells. *Clin Cancer Res* **16**, 3485-3494 (2010).

84. Yi, J.S. *et al.* Immune Activation in Early-Stage Non-Small Cell Lung Cancer Patients Receiving Neoadjuvant Chemotherapy Plus Ipilimumab. *Clin Cancer Res* **23**, 7474-7482 (2017).

85. Ng Tang, D. *et al.* Increased frequency of ICOS+ CD4 T cells as a pharmacodynamic biomarker for anti-CTLA-4 therapy. *Cancer Immunol Res* **1**, 229-234 (2013).

86. Carthon, B.C. *et al.* Preoperative CTLA-4 blockade: tolerability and immune monitoring in the setting of a presurgical clinical trial. *Clin Cancer Res* **16**, 2861-2871 (2010).

87. Rochigneux, P. *et al.* Mass cytometry reveals classical monocytes, NK cells and ICOS+ CD4+ T cells associated with pembrolizumab efficacy in lung cancer patients. *Clin Cancer Res* (2022).

88. Fu, T., He, Q. & Sharma, P. The ICOS/ICOSL Pathway Is Required for Optimal Antitumor Responses Mediated by Anti–CTLA-4 Therapy. *Cancer Research* **71**, 5445-5454 (2011).

89. Fan, X., Quezada, S.A., Sepulveda, M.A., Sharma, P. & Allison, J.P. Engagement of the ICOS pathway markedly enhances efficacy of CTLA-4 blockade in cancer immunotherapy. *J Exp Med* **211**, 715-725 (2014).

90. Martin-Orozco, N. *et al.* Melanoma cells express ICOS ligand to promote the activation and expansion of T-regulatory cells. *Cancer Res* **70**, 9581-9590 (2010).

91. Han, Y. *et al.* Acute Myeloid Leukemia Cells Express ICOS Ligand to Promote the Expansion of Regulatory T Cells. *Front Immunol* **9**, 2227 (2018).

92. Conrad, C. *et al.* Plasmacytoid dendritic cells promote immunosuppression in ovarian cancer via ICOS costimulation of Foxp3(+) T-regulatory cells. *Cancer Res* **72**, 5240-5249 (2012).

93. Wang, B. *et al.* Expression of ICOSL is associated with decreased survival in invasive breast cancer. *PeerJ* **7**, e6903 (2019).

94. Solinas, C., Gu-Trantien, C. & Willard-Gallo, K. The rationale behind targeting the ICOS-ICOS ligand costimulatory pathway in cancer immunotherapy. *ESMO Open* **5** (2020).

95. Panneton, V., Bagherzadeh Yazdchi, S., Witalis, M., Chang, J. & Suh, W.K. ICOS Signaling Controls Induction and Maintenance of Collagen-Induced Arthritis. *J Immunol* **200**, 3067-3076 (2018).

96. Kedl, R.M. *et al.* CD40 stimulation accelerates deletion of tumor-specific CD8(+) T cells in the absence of tumor-antigen vaccination. *Proc Natl Acad Sci U S A* **98**, 10811-10816 (2001).

97. Stuart, T. *et al.* Comprehensive Integration of Single-Cell Data. *Cell* **177**, 1888-1902.e1821 (2019).

98. Waltman, L. & van Eck, N.J. A smart local moving algorithm for large-scale modularity-based community detection. *The European Physical Journal B* **86**, 471 (2013).

99. McInnes, L., Healy, J. & Melville, J. Umap: Uniform manifold approximation and projection for dimension reduction. *arXiv preprint arXiv:1802.03426* (2018).

100. Vogel, C. & Marcotte, E.M. Insights into the regulation of protein abundance from proteomic and transcriptomic analyses. *Nat Rev Genet* **13**, 227-232 (2012).

101. Maier, T., Güell, M. & Serrano, L. Correlation of mRNA and protein in complex biological samples. *FEBS Lett* **583**, 3966-3973 (2009).

102. Terabe, M. & Berzofsky, J.A. Tissue-Specific Roles of NKT Cells in Tumor Immunity. *Front Immunol* **9**, 1838 (2018).

103. Liu, Y. & Zhang, C. The Role of Human γδ T Cells in Anti-Tumor Immunity and Their Potential for Cancer Immunotherapy. *Cells* **9** (2020).

104. Beltra, J.C. *et al.* Developmental Relationships of Four Exhausted CD8(+) T Cell Subsets Reveals Underlying Transcriptional and Epigenetic Landscape Control Mechanisms. *Immunity* **52**, 825-841.e828 (2020).

105. Li, J., He, Y., Hao, J., Ni, L. & Dong, C. High Levels of Eomes Promote Exhaustion of Anti-tumor CD8(+) T Cells. *Front Immunol* **9**, 2981 (2018).

106. Fuertes Marraco, S.A., Neubert, N.J., Verdeil, G. & Speiser, D.E. Inhibitory Receptors Beyond T Cell Exhaustion. *Front Immunol* **6**, 310 (2015).

107. Agata, Y. *et al.* Expression of the PD-1 antigen on the surface of stimulated mouse T and B lymphocytes. *Int Immunol* **8**, 765-772 (1996).

108. Walunas, T.L. *et al.* CTLA-4 can function as a negative regulator of T cell activation. *Immunity* **1**, 405-413 (1994).

109. Legat, A., Speiser, D.E., Pircher, H., Zehn, D. & Fuertes Marraco, S.A. Inhibitory Receptor Expression Depends More Dominantly on Differentiation and Activation than "Exhaustion" of Human CD8 T Cells. *Front Immunol* **4**, 455 (2013).

110. Intlekofer, A.M. *et al.* Effector and memory CD8+ T cell fate coupled by T-bet and eomesodermin. *Nat Immunol* **6**, 1236-1244 (2005).

111. Banerjee, A. *et al.* Cutting edge: The transcription factor eomesodermin enables CD8+ T cells to compete for the memory cell niche. *J Immunol* **185**, 4988-4992 (2010).

112. Reiser, J., Sadashivaiah, K., Furusawa, A., Banerjee, A. & Singh, N. Eomesodermin driven IL-10 production in effector CD8(+) T cells promotes a memory phenotype. *Cell Immunol* **335**, 93-102 (2019).

113. Chaput, N. *et al.* Regulatory T cells prevent CD8 T cell maturation by inhibiting CD4 Th cells at tumor sites. *J Immunol* **179**, 4969-4978 (2007).

114. La Manno, G. *et al.* RNA velocity of single cells. *Nature* **560**, 494-498 (2018).

115. Bergen, V., Lange, M., Peidli, S., Wolf, F.A. & Theis, F.J. Generalizing RNA velocity to transient cell states through dynamical modeling. *Nature Biotechnology* **38**, 1408-1414 (2020).

116. Bergen, V., Soldatov, R.A., Kharchenko, P.V. & Theis, F.J. RNA velocity-current challenges and future perspectives. *Mol Syst Biol* **17**, e10282 (2021).

117. Sakaguchi, S., Sakaguchi, N., Asano, M., Itoh, M. & Toda, M. Immunologic self-tolerance maintained by activated T cells expressing IL-2 receptor alpha-chains (CD25). Breakdown of a single mechanism of self-tolerance causes various autoimmune diseases. *J Immunol* **155**, 1151-1164 (1995).

118. Dioszeghy, V. *et al.* Differences in phenotype, homing properties and suppressive activities of regulatory T cells induced by epicutaneous, oral or sublingual immunotherapy in mice sensitized to peanut. *Cell Mol Immunol* **14**, 770-782 (2017).

119. Ferhat, M. *et al.* Lack of protective effect of CCR3 blockade during experimental colitis may be related to CCR3 expression by colonic Tregs. *Clin Transl Med* **11**, e455 (2021).

120. Vilgelm, A.E. & Richmond, A. Chemokines Modulate Immune Surveillance in Tumorigenesis, Metastasis, and Response to Immunotherapy. *Front Immunol* **10**, 333 (2019).

121. Reyes, N., Figueroa, S., Tiwari, R. & Geliebter, J. CXCL3 Signaling in the Tumor Microenvironment. *Adv Exp Med Biol* **1302**, 15-24 (2021).

122. Harrison, O.J. *et al.* Epithelial-derived IL-18 regulates Th17 cell differentiation and Foxp3^{+} Treg cell function in the intestine. *Mucosal Immunol* **8**, 1226-1236 (2015).

123. Oertli, M. *et al.* DC-derived IL-18 drives Treg differentiation, murine Helicobacter pylori-specific immune tolerance, and asthma protection. *J Clin Invest* **122**, 1082-1096 (2012).